



# TECH BRIEFS

NATIONAL AERONAUTICS AND SPACE ADMINISTRATION

-  **Technology Focus**
-  **Electronics/Computers**
-  **Software**
-  **Materials**
-  **Mechanics**
-  **Machinery/Automation**
-  **Manufacturing**
-  **Bio-Medical**
-  **Physical Sciences**
-  **Information Sciences**
-  **Books and Reports**



## INTRODUCTION

Tech Briefs are short announcements of innovations originating from research and development activities of the National Aeronautics and Space Administration. They emphasize information considered likely to be transferable across industrial, regional, or disciplinary lines and are issued to encourage commercial application.

### Availability of NASA Tech Briefs and TSPs

Requests for individual Tech Briefs or for Technical Support Packages (TSPs) announced herein should be addressed to

#### National Technology Transfer Center

Telephone No. (800) 678-6882 or via World Wide Web at [www2.nttc.edu/leads/](http://www2.nttc.edu/leads/)

Please reference the control numbers appearing at the end of each Tech Brief. Information on NASA's Commercial Technology Team, its documents, and services is also available at the same facility or on the World Wide Web at [www.nctn.hq.nasa.gov](http://www.nctn.hq.nasa.gov).

Innovative Partnerships Offices are located at NASA field centers to provide technology-transfer access to industrial users. Inquiries can be made by contacting NASA field centers and Mission Directorates listed below.

## NASA Field Centers and Program Offices

#### Ames Research Center

Lisa L. Lockyer  
(650) 604-1754  
[lisa.l.lockyer@nasa.gov](mailto:lisa.l.lockyer@nasa.gov)

#### Dryden Flight Research Center

Gregory Poteat  
(661) 276-3872  
[greg.poteat@dfrc.nasa.gov](mailto:greg.poteat@dfrc.nasa.gov)

#### Goddard Space Flight Center

Nona Cheeks  
(301) 286-5810  
[Nona.K.Cheeks.1@nasa.gov](mailto:Nona.K.Cheeks.1@nasa.gov)

#### Jet Propulsion Laboratory

Ken Wolfenbarger  
(818) 354-3821  
[james.k.wolfenbarger@jpl.nasa.gov](mailto:james.k.wolfenbarger@jpl.nasa.gov)

#### Johnson Space Center

Helen Lane  
(713) 483-7165  
[helen.w.lane@nasa.gov](mailto:helen.w.lane@nasa.gov)

#### Kennedy Space Center

Jim Aliberti  
(321) 867-6224  
[Jim.Aliberti-1@nasa.gov](mailto:Jim.Aliberti-1@nasa.gov)

#### Langley Research Center

Ray P. Turcotte  
(757) 864-8881  
[r.p.turcotte@larc.nasa.gov](mailto:r.p.turcotte@larc.nasa.gov)

#### John H. Glenn Research Center at Lewis Field

Robert Lawrence  
(216) 433-2921  
[robert.f.lawrence@nasa.gov](mailto:robert.f.lawrence@nasa.gov)

#### Marshall Space Flight Center

Vernotto McMillan  
(256) 544-2615  
[vernotto.mcmillan@msfc.nasa.gov](mailto:vernotto.mcmillan@msfc.nasa.gov)

#### Stennis Space Center

John Bailey  
(228) 688-1660  
[john.w.bailey@nasa.gov](mailto:john.w.bailey@nasa.gov)

#### NASA Mission Directorates

At NASA Headquarters there are four Mission Directorates under which there are seven major program offices that develop and oversee technology projects of potential interest to industry:

##### Carl Ray

Small Business Innovation Research Program (SBIR) & Small Business Technology Transfer Program (STTR)  
(202) 358-4652  
[carl.g.ray@nasa.gov](mailto:carl.g.ray@nasa.gov)

##### Frank Schowengerdt

Innovative Partnerships Program (Code TD)  
(202) 358-2560  
[fschowen@hq.nasa.gov](mailto:fschowen@hq.nasa.gov)

##### John Mankins

Exploration Systems Research and Technology Division  
(202) 358-4659  
[john.c.mankins@nasa.gov](mailto:john.c.mankins@nasa.gov)

##### Terry Hertz

Aeronautics and Space Mission Directorate  
(202) 358-4636  
[thertz@mail.hq.nasa.gov](mailto:thertz@mail.hq.nasa.gov)

##### Glen Mucklow

Mission and Systems Management Division (SMD)  
(202) 358-2235  
[gmucklow@mail.hq.nasa.gov](mailto:gmucklow@mail.hq.nasa.gov)

##### Granville Paules

Mission and Systems Management Division (SMD)  
(202) 358-0706  
[gpaules@mtpe.hq.nasa.gov](mailto:gpaules@mtpe.hq.nasa.gov)

##### Gene Trinh

Human Systems Research and Technology Division (ESMD)  
(202) 358-1490  
[eugene.h.trinh@nasa.gov](mailto:eugene.h.trinh@nasa.gov)

##### John Rush

Space Communications Office (SOMD)  
(202) 358-4819  
[john.j.rush@nasa.gov](mailto:john.j.rush@nasa.gov)





# TECH BRIEFS

NATIONAL AERONAUTICS AND SPACE ADMINISTRATION



## 5 Technology Focus: Fastening/Joining

- 5 Fastener Starter
- 5 Multifunctional Deployment Hinges Rigidified by Ultraviolet
- 6 Temperature-Controlled Clamping and Releasing Mechanism



## 7 Electronics/Computers

- 7 Long-Range Emergency Preemption of Traffic Lights
- 7 High-Efficiency Microwave Power Amplifier
- 8 Improvements of ModalMax High-Fidelity Piezoelectric Audio Device
- 8 Alumina or Semiconductor Ribbon Waveguides at 30 to 1,000 GHz
- 9 HEMT Frequency Doubler With Output at 300 GHz
- 10 Single-Chip FPGA Azimuth Pre-Filter for SAR



## 13 Software

- 13 Autonomous Navigation by a Mobile Robot
- 13 Software Would Largely Automate Design of Kalman Filter
- 13 Predicting Flows of Rarefied Gases
- 13 Centralized Planning for Multiple Exploratory Robots
- 13 Electronic Router



## 15 Mechanics

- 15 Piezo-Operated Shutter Mechanism Moves 1.5 cm
- 16 Two SMA-Actuated Miniature Mechanisms



## 19 Machinery/Automation

- 19 Vortobots
- 20 Ultrasonic/Sonic Jackhammer



## 21 Bio-Medical

- 21 Removing Pathogens Using Nano-Ceramic-Fiber Filters
- 21 Satellite-Derived Management Zones



## 23 Physical Sciences

- 23 Digital Equivalent Data System for XRF Labeling of Objects
- 24 Identifying Objects via Encased X-Ray-Fluorescent Materials — the Bar Code Inside
- 25 Vacuum Attachment for XRF Scanner
- 26 Simultaneous Conoscopic Holography and Raman Spectroscopy
- 27 Adding GaAs Monolayers to InAs Quantum-Dot Lasers on (001) InP
- 28 Vibrating Optical Fibers To Make Laser Speckle Disappear



## 29 Information Sciences

- 29 Adaptive Filtering Using Recurrent Neural Networks
- 30 Applying Standard Interfaces to a Process-Control Language

This document was prepared under the sponsorship of the National Aeronautics and Space Administration. Neither the United States Government nor any person acting on behalf of the United States Government assumes any liability resulting from the use of the information contained in this document, or warrants that such use will be free from privately owned rights.





## Fastener Starter

**This tool is superior to prior screw and nut starters.**

*John F. Kennedy Space Center, Florida*

The Fastener Starter is a creative solution to prevent the loss of small fasteners during their installation. This is the only currently available tool that can firmly grip and hold a single screw, bolt, nut, washer, spacer, or any combination of these parts. Other commercially available fastener starters are unable to accommodate a variety of parts simultaneously. The Fastener Starter is a more capable and easier tool to use than prior tools. Its compact size allows it to be used effectively in cramped, difficult-to-see locations. Its design also allows it to be used with or without handles and extenders in other difficult-to-reach locations. It provides better protection against cross threading and loss of fasteners and associated parts. The Fastener Starter is non-magnetic and does not off-gas, thus meeting flight hardware requirements.

The Fastener Starter incorporates a combination of features of several commercially available tools, providing an improved means of installing small fasteners. The Fastener Starter includes a custom molded insert that can be removed easily and replaced with a con-

ventional tool bit (e.g., a screwdriver or hex-driver bit). When used with the insert, the Fastener Starter prevents cross threading and damage to internal threaded holes. This is achieved by allowing the fastener to slip within the tool insert when used without a conventional tool bit. Alternatively, without the insert and with a tool bit, the Fastener Starter can torque a fastener. The Fastener Starter has a square recess hole that accepts a conventional square drive handle or extension to accommodate a variety of applications by providing flexibility in handle style and length.

In a typical operation sequence, the user opens the tool, places a screw, screw/washer combination, nut, or nut/washer combination against and within the insert (or tool bit), and closes the tool, which firmly grasps the hardware. The user then guides the fastener to its destination and turns the tool to attach the fastener. Once the fastener is attached, the user simply pulls back on the tool to open it and release the fastener.

In tests that involved the installation of more than 300 screws and washers, in

several orientations and at different distances from the users, the tool did not drop any parts. In addition, most of the users participating in the tests expressed their preference to use this tool rather than only their hands to start a fastener installation.

*This work was done by Faith Chandler, Harry Garton, Bill Valentino, and Mike Amett of The Boeing Company for Kennedy Space Center.*

*Title to this invention, covered by U.S. Patent No. 6,606,924, has been waived under the provisions of the National Aeronautics and Space Act {42 U.S.C. 2457(f)}, to The Boeing Company. Inquiries concerning licenses for its commercial development should be addressed to:*

*Terrance Mason, Boeing Patent Licensing Professional*

*Boeing Management Co.*

*Mail Stop 1650-7002*

*15460 Laguna Canyon Road*

*Irvine, CA 92618*

*Phone No.: (949) 790-1331*

*E-mail: terrance.mason@boeing.com*

*Refer to KSC-12224, volume and number of this NASA Tech Briefs issue, and the page number.*

## Multifunctional Deployment Hinges Rigidified by Ultraviolet

**These hinges provide both structural support and electrical connections.**

*John H. Glenn Research Center, Cleveland, Ohio*

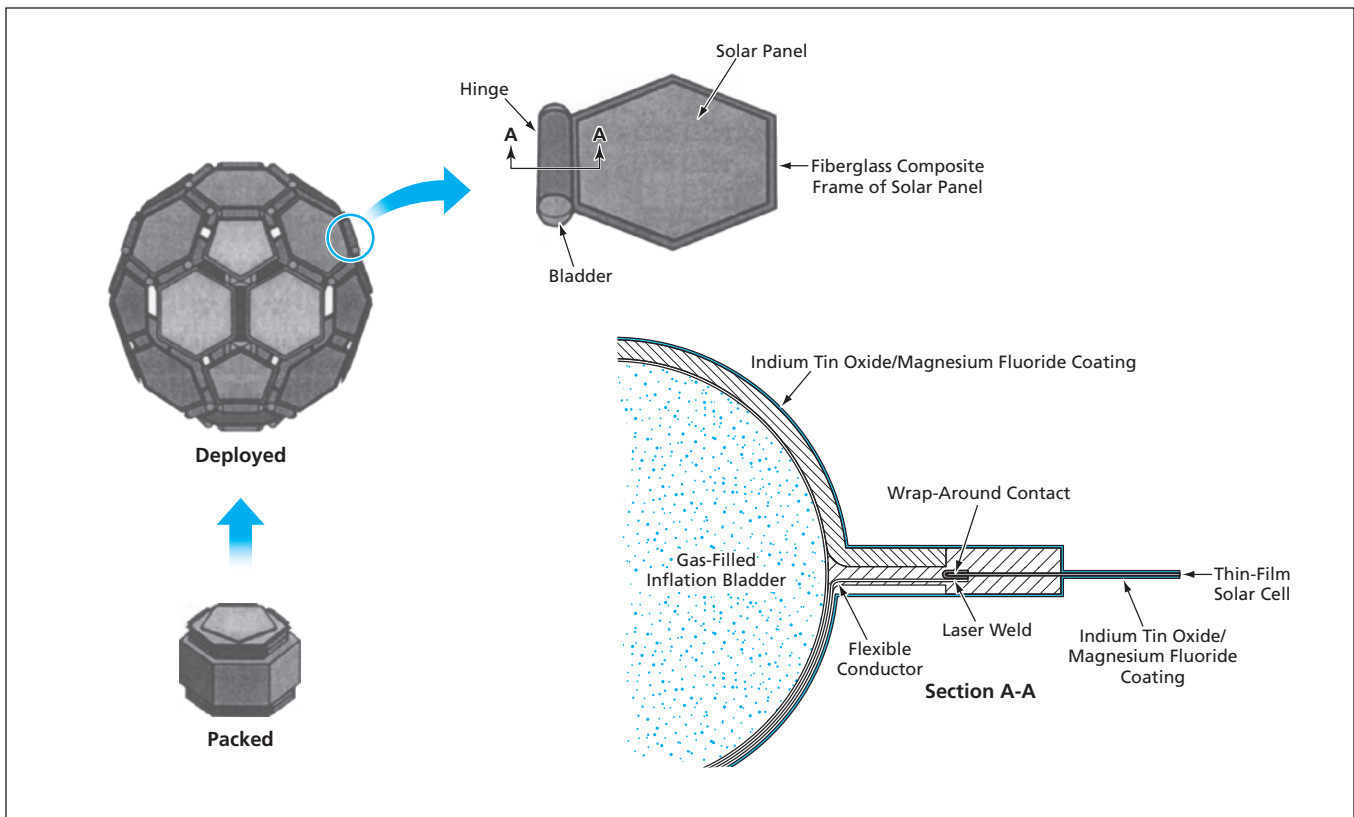
Multifunctional hinges have been developed for deploying and electrically connecting panels comprising planar arrays of thin-film solar photovoltaic cells. In the original intended application of these hinges, the panels would be facets of a 32-sided (and approximately spherical) polyhedral microsatellite (see figure), denoted a PowerSphere, that would be delivered to orbit in a compact folded configuration, then deployed by expansion of gas in inflation bladders. Once deployment was complete, the hinges would be

rigidified to provide structural connections that would hold the panels in their assigned relative positions without backlash. Such hinges could also be used on Earth for electrically connecting and structurally supporting solar panels that are similarly shipped in compact form and deployed at their destinations.

As shown in section A-A in the figure, a hinge of this type is partly integrated with an inflation bladder and partly integrated with the frame of a solar panel. During assembly of the

hinge, strip extensions from a flexible circuit harness on the bladder are connected to corresponding thin-film conductors on the solar panel by use of laser welding and wrap-around contacts. The main structural component of the hinge is a layer of glass fiber impregnated with an ultraviolet-curable resin. After deployment, exposure to ultraviolet light from the Sun cures the resin, thereby rigidifying the hinge.

1. In the original intended satellite application, it would protect the under-



A Polyhedral Assembly of Solar Panels would be deployed from compact stowage in two stacks, each containing ten hexagonal and six pentagonal panels. The deployment hinges between the panels would be key components that would accommodate the unfolding during deployment, hold the panels in their proper alignments after deployment, and provide electrical connections for the panels.

- lying polymeric components against erosion by monatomic oxygen in low orbit around the Earth;
- 2. It is sufficiently ultraviolet-transmissive to enable curing of the resin by exposure to ultraviolet light from the Sun or another suitable source;
- 3. It exhibits improved (relative to prior coating materials) transmittance of visible light for collection by solar cells; and

4. It resists darkening under long-term exposure to ultraviolet light.

This work was done by Thomas W. Kerslake of **Glenn Research Center**; Edward J. Simburger, James Matusmoto, Thomas W. Giants, and Alexander Garcia of *The Aerospace Corporation*; Alan Perry, Suraj Rawal, and Craig Marshall of *Lockheed Martin Corp.*; and John Kun Hung Lin, Jonathan Robert Day, and Stephen

*Emerson Scarborough of ILC Dover, Inc.* Further information is contained in a TSP (see page 1).

Inquiries concerning rights for the commercial use of this invention should be addressed to NASA Glenn Research Center, Commercial Technology Office, Attn: Steve Fedor, Mail Stop 4-8, 21000 Brookpark Road, Cleveland, Ohio 44135. Refer to LEW-17476-1.

## Temperature-Controlled Clamping and Releasing Mechanism

NASA's Jet Propulsion Laboratory, Pasadena, California

A report describes the development of a mechanism that automatically clamps upon warming and releases upon cooling between temperature limits of  $\approx 180$  K and  $\approx 293$  K. The mechanism satisfied a need specific to a program that involved repeated excursions of a spectrometer between a room-temperature atmospheric environment and a cryogenic vacuum testing environment. The mechanism was also to be utilized in the intended application of the spectrometer, in which

the spectrometer would be clamped for protection during launch of a spacecraft and released in the cold of outer space to allow it to assume its nominal configuration for scientific observations. The mechanism is passive in the sense that its operation does not depend on a control system and does not require any power other than that incidental to heating and cooling. The clamping and releasing action is effected by bolt-preloaded stacks of shape-memory-alloy (SMA)

cylinders. In designing this mechanism, as in designing other, similar SMA mechanisms, it was necessary to account for the complex interplay among thermal expansion, elastic and inelastic deformation under load, and SMA thermomechanical properties.

This work was done by David Rosing and Virginia Ford of Caltech for NASA's Jet Propulsion Laboratory. Further information is contained in a TSP (see page 1). Further information is contained in a TSP (see page 1). NPO-40541



## Long-Range Emergency Preemption of Traffic Lights

Addition of a forwarding system could improve preemption performance.

NASA's Jet Propulsion Laboratory, Pasadena, California

A forwarding system could prove beneficial as an addition to an electronic communication-and-control system that automatically modifies the switching of traffic lights to give priority to emergency vehicles. A system to which the forwarding system could be added could be any of a variety of emergency traffic-signal-preemption systems: these include systems now used in some municipalities as well as advanced developmental systems described in several NASA Tech Briefs articles in recent years.

Because of a variety of physical and design limitations, emergency traffic-signal-preemption systems now in use are often limited in range to only one intersection at a time: in a typical system, only the next, closest intersection is preempted for an emergency vehicle. Simulations of gridlock have shown that such systems offer minimal advantages and can even cause additional delays.

In analogy to what happens in fluid dynamics, the forwarding system insures that flow at a given location is sustained by guaranteeing downstream flow along the predicted route (typically a main artery) and intersecting routes (typically, side streets). In simplest terms, the forwarding system starts by taking note of any preemption issued by the preemption system to which it has been added. The forwarding system predicts which other intersections could be encountered by the emergency vehicle downstream of the newly preempted intersection. The system then forwards preemption triggers to those intersections.

Beyond affording a right of way for the emergency vehicle at every intersection that lies ahead along any likely route from the current position of the vehicle, the forwarding system also affords the benefit of clearing congested roads far ahead of the vehicle. In a metropolitan

environment with heavy road traffic, forwarding of preemption triggers could greatly enhance the performance of a pre-existing preemption system.

*This work was done by Aaron Bachelder of Caltech for NASA's Jet Propulsion Laboratory. Further information is contained in a TSP (see page 1).*

*In accordance with Public Law 96-517, the contractor has elected to retain title to this invention. Inquiries concerning rights for its commercial use should be addressed to:*

*Innovative Technology Assets Management  
JPL*

*Mail Stop 202-233*

*4800 Oak Grove Drive*

*Pasadena, CA 91109-8099*

*(818) 354-2240*

*E-mail: iaoffice@jpl.nasa.gov*

*Refer to NPO-40492, volume and number of this NASA Tech Briefs issue, and the page number.*

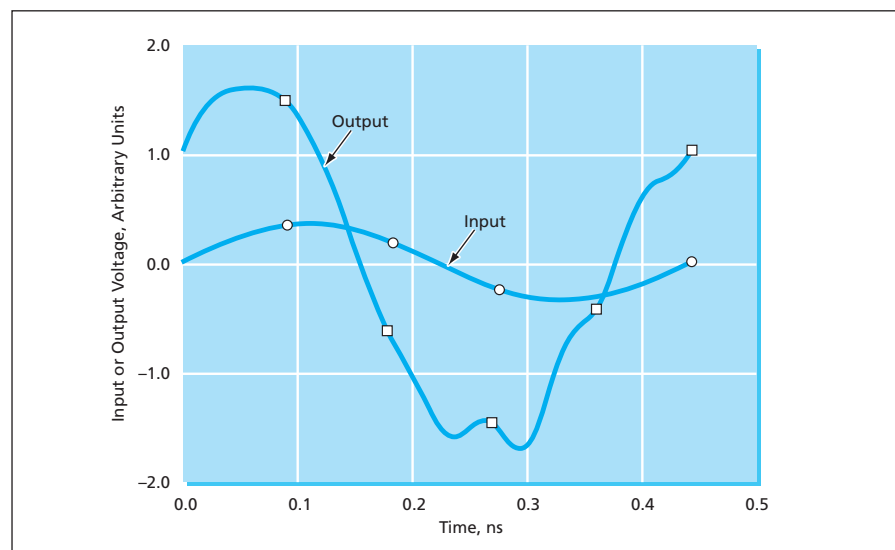
## High-Efficiency Microwave Power Amplifier

High efficiency is achieved through class-D operation.

Marshall Space Flight Center, Alabama

A high-efficiency power amplifier that operates in the S band (frequencies of the order of a few gigahertz) utilizes transistors operating under class-D bias and excitation conditions. Class-D operation has been utilized at lower frequencies, but, until now, has not been exploited in the S band.

Nominally, in class D operation, a transistor is switched rapidly between "on" and "off" states so that at any given instant, it sustains either high current or high voltage, but not both at the same time. In the ideal case of zero "on" resistance, infinite "off" resistance, zero inductance and capacitance, and perfect switching, the output signal would be a perfect square wave. Relative to the traditional classes A, B, and C of amplifier operation, class D offers the potential to achieve greater power efficiency. In addition, relative to class-A amplifiers, class-D



The **Output Waveform** of the amplifier is of an intermediate form achieved in an effort to obtain a square-wave output from a sinusoidal input.

Measurement	Input Stage	Driver Stage	Final Stage
Input Voltage Standing-Wave Ratio	1.0023:1	1.9:1	33:1
Gain, dB	13.3	8.8	9.6
DC-to-RF Efficiency, Percent	54.2	42.6	58.6
Power-Added Efficiency, Percent	51.7	36.9	52.2

Several Measurements were made on each amplifier stage to characterize its performance.

amplifiers are less likely to go into oscillation.

In order to design this amplifier, it was necessary to derive mathematical models of microwave power transistors for incorporation into a larger mathe-

tical model for computational simulation of the operation of a class-D microwave amplifier. The design incorporates state-of-the-art switching techniques applicable only in the microwave frequency range. Another major novel

feature is a transmission-line power splitter/combiner designed with the help of phasing techniques to enable an approximation of a square-wave signal (which is inherently a wideband signal) to propagate through what would, if designed in a more traditional manner, behave as a more severely band-limited device (see figure).

The amplifier includes an input, a driver, and a final stage. Each stage contains a pair of GaAs-based field-effect transistors biased in class D. The input signal can range from -10 to +10 dBm into a 50-ohm load. The table summarizes the performances of the three stages.

*This work was done by William H. Sims of Marshall Space Flight Center.*

*This invention has been patented by NASA (U.S. Patent No. 6,388,512). Inquiries concerning nonexclusive or exclusive license for its commercial development should be addressed to Sammy Nabors, MSFC Commercialization Assistance Lead, at (256) 544-5226 or sammy.a.nabors@nasa.gov. Refer to MFS-31455.*

## Improvements of ModalMax High-Fidelity Piezoelectric Audio Device

Langley Research Center, Hampton, Virginia

ModalMax audio speakers have been enhanced by innovative means of tailoring the vibration response of thin piezoelectric plates to produce a high-fidelity audio response. The ModalMax audio speakers are 1 mm in thickness. The device completely supplants the need to have a separate driver and speaker cone. ModalMax speakers can perform the same applications of cone speakers, but unlike cone speakers, ModalMax speakers can function in harsh environ-

ments such as high humidity or extreme wetness. New design features allow the speakers to be completely submerged in salt water, making them well suited for maritime applications. The sound produced from the ModalMax audio speakers has sound spatial resolution that is readily discernable for headset users. [The ModalMax product line was described in "High-Fidelity Piezoelectric Audio Device" (LAR-15959), *NASA Tech Briefs*, Vol. 27, No. 8 (August

2003), page 36.] Other improvements of the ModalMax audio speakers include methods to reduce size, reduce power demand, and increase audio fidelity by increasing vibrational responses at the low and high ends of the audio frequency range.

*This work was done by Stanley E. Woodard of Langley Research Center. Further information is contained in a TSP (see page 1). LAR-16321-1*

## Alumina or Semiconductor Ribbon Waveguides at 30 to 1,000 GHz

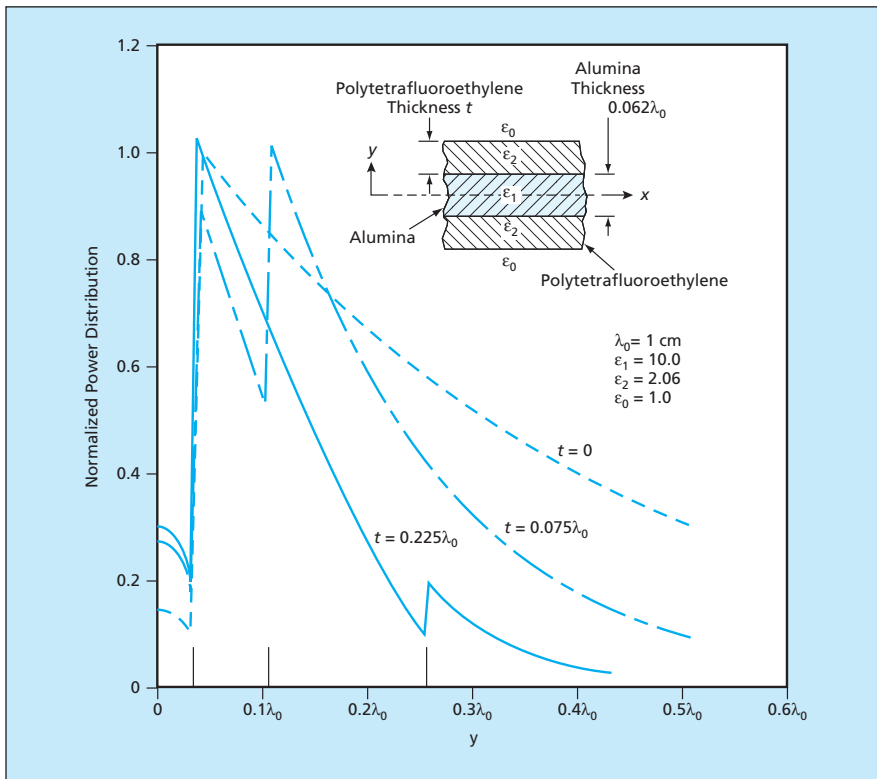
The waveguides would be configured to exploit low-loss electromagnetic modes.

NASA's Jet Propulsion Laboratory, Pasadena, California

Ribbon waveguides made of alumina or of semiconductors (Si, InP, or GaAs) have been proposed as low-loss transmission lines for coupling electronic components and circuits that operate at frequencies from 30 to 1,000 GHz. In addition to low losses (and a concomi-

tant ability to withstand power levels higher than would otherwise be possible), the proposed ribbon waveguides would offer the advantage of compatibility with the materials and structures now commonly incorporated into integrated circuits.

Heretofore, low-loss transmission lines for this frequency range have been unknown, making it necessary to resort to designs that, variously, place circuits and components to be coupled in proximity of each other and/or provide for coupling via free space through bulky



**Normalized Power Densities** were computed for a dominant  ${}_{e}HE_{11}$  mode on a ribbon waveguide made of alumina (having assumed relative permittivity of 10), both uncoated and coated with various thicknesses polytetrafluoroethylene (having assumed relative permittivity of 2.06). The unit of thickness used in the computations was the free-space wavelength,  $\lambda_0$ .

and often lossy optical elements. Even chip-to-chip interconnections have been problematic in this frequency range. Metal wave-guiding structures (e.g., microstriplines and traditional waveguides) are not suitable for this frequency range because the skin depths of electromagnetic waves in this frequency range are so small as to give rise to high losses. Conventional rod-type dielectric waveguide structures are also not suitable for this frequency range because dielectric materials, including ones that exhibit ultralow losses at lower frequencies, exhibit significant losses in this frequency range.

Unlike microstripline structures or metallic waveguides, the proposed ribbon waveguides would be free of metal and would therefore not be subject to skin-depth losses. Moreover, although they would be made of materials that are moderately lossy in the frequency range of interest, the proposed ribbon waveguides would cause the propagating electromagnetic waves to configure themselves in a manner that minimizes losses.

The basic principle for minimizing losses was described in "Ceramic Ribbons as Waveguides at Millimeter Wavelengths" (NPO-21001), *NASA Tech Briefs*, Vol. 25, No. 4 (April 2001), page 49. To

recapitulate: The cross-sectional geometry of a waveguide ribbon would be chosen in consideration of the permittivity of the ribbon material to support an electromagnetic mode in which most of the energy would propagate, parallel to the ribbon, through the adjacent free space and only a small fraction would propagate within the ribbon. As a result, the interaction of the propagating wave with the dielectric core (and thus the attenuation) would be minimal.

For straight runs, the ribbon waveguides would be uncoated. However, since most of the guided power would be carried in the nearly lossless air just outside the ribbon, a significant portion of the guided power could be expected to be radiated (and thus lost) where the guiding ribbon was sharply curved (for example, to bend it around a corner). In such a case, the short length of the ribbon containing the curve could be coated with a layer of a polymer having a suitable permittivity intermediate between that of air and that of the ribbon, so that most of the power would not be radiated but would remain confined within the polymer layer (see figure) while propagating around the corner.

*This work was done by Cavour Yeh, Daniel Rascoe, Fred Shimabukuro, Michael Tope, and Peter Siegel of Caltech for NASA's Jet Propulsion Laboratory. Further information is contained in a TSP (see page 1).*

*In accordance with Public Law 96-517, the contractor has elected to retain title to this invention. Inquiries concerning rights for its commercial use should be addressed to:*

*Innovative Technology Assets Management  
JPL Mail Stop 202-233  
4800 Oak Grove Drive  
Pasadena, CA 91109-8099  
(818) 354-2240*

*E-mail: iaoffice@jpl.nasa.gov  
Refer to NPO-30339, volume and number of this NASA Tech Briefs issue, and the page number.*

## HEMT Frequency Doubler With Output at 300 GHz

**This is the highest-frequency HEMT doubler reported to date.**

*NASA's Jet Propulsion Laboratory, Pasadena, California*

An active frequency doubler in the form of an InP-based monolithic microwave integrated circuit (MMIC) containing a high-electron-mobility transistor (HEMT) has been demonstrated in operation at output frequencies in the vicinity of 300 GHz. This is the highest-

frequency HEMT doubler reported to date, the next-highest-frequency active HEMT doubler having been previously reported to operate at 180 GHz. While the output power of this frequency doubler is less than that of a typical Schottky diode, this frequency doubler is consid-

ered an intermediate product of a continuing effort to realize the potential of active HEMT frequency doublers to operate with conversion efficiencies greater than those of passive diode frequency doublers. An additional incentive for developing active HEMT frequency dou-

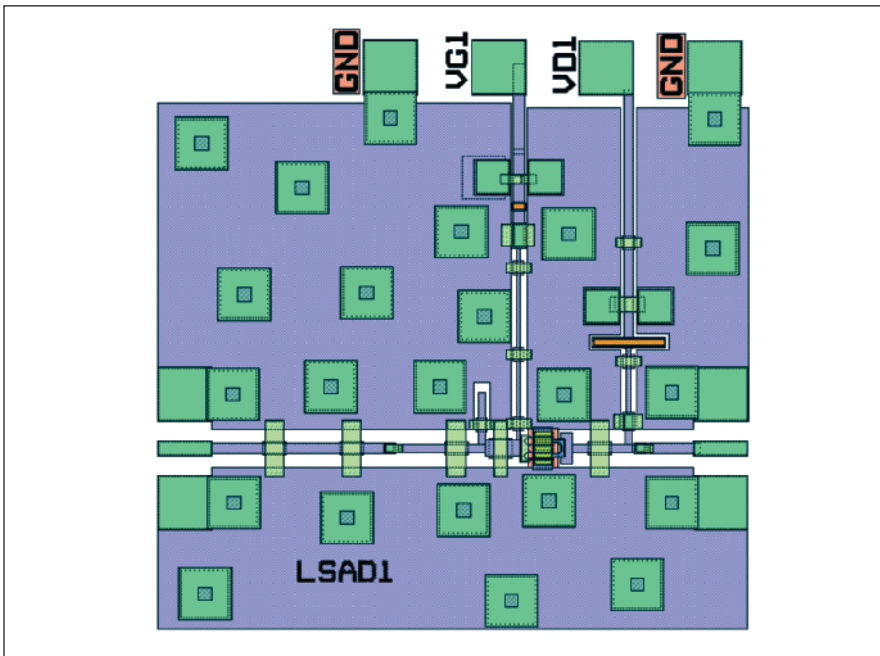


Figure 1. This MMIC embodies an active frequency doubler rated for a nominal output frequency of about 300 GHz.

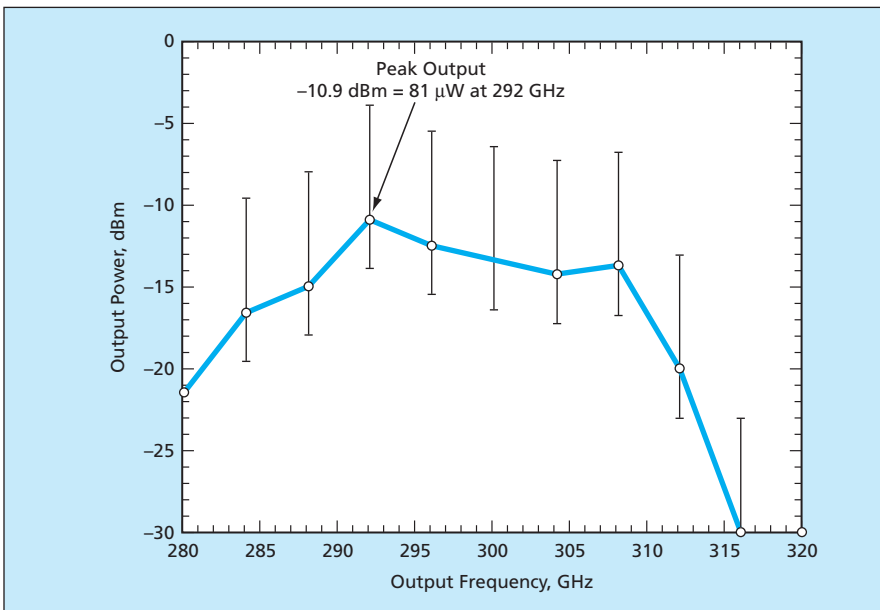


Figure 2. The Output Power of the MMIC of Figure 1 was measured at several output frequencies from 280 to 316 GHz.

blers lies in the fact that they can be integrated with amplifiers, oscillators, and other circuitry on MMIC chips.

The circuitry of the doubler MMIC (see Figure 1) features grounded coplanar waveguides. Air bridges and vias are used to make contact with the ground plane. The HEMT is biased for Class-A operation (in which current is conducted throughout each cycle of oscillation), which would ordinarily be better suited to linear amplification than to frequency doubling. Ordinarily, class-B operation (in which current is conducted during about half of each cycle of oscillation) would be more suitable for frequency doubling because of the essential non-linearity of partial-cycle conduction. The reason for the unusual choice of class A was that computational simulations had shown that in this case, the efficiency in class B would be less than in class A.

The input matching circuit of this doubler includes transmission lines that afford a good impedance match at the fundamental frequency, plus an open stub to prevent leakage of the second harmonic through the input terminals. The output circuit was designed to suppress the fundamental while providing a good match for the second harmonic.

In a test, this doubler was driven by an input signal at frequencies from 140 to 158 GHz and its output at the corresponding second-harmonic frequencies of 280 to 316 GHz was measured by means of a power meter connected to the MMIC via waveguide wafer probes and a high-pass (fundamental-suppressing) waveguide. The results of this test are summarized in Figure 2.

*This work was done by Lorene Samoska and Jean Bruston of Caltech for NASA's Jet Propulsion Laboratory. Further information is contained in a TSP (see page 1). NPO-30581*

## Single-Chip FPGA Azimuth Pre-Filter for SAR

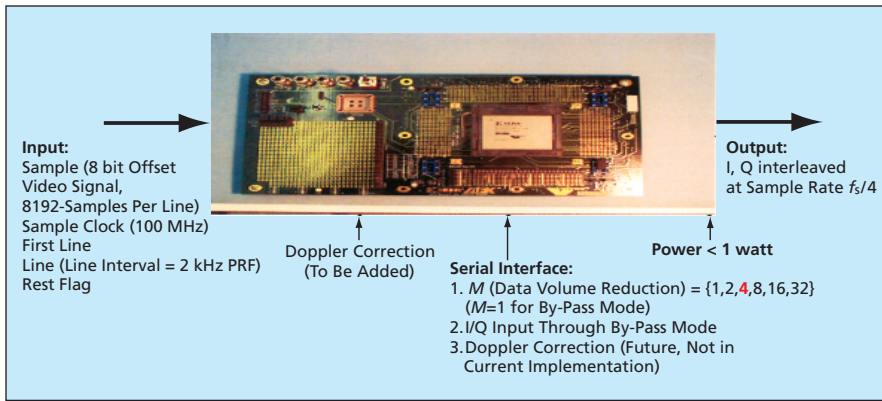
Range resolution is reduced by a selectable factor to reduce the volume of data.

NASA's Jet Propulsion Laboratory, Pasadena, California

A field-programmable gate array (FPGA) on a single lightweight, low-power integrated-circuit chip has been developed to implement an azimuth pre-filter (AzPF) for a synthetic-aperture radar (SAR) system. The AzPF is

needed to enable more efficient use of data-transmission and data-processing resources: In broad terms, the AzPF reduces the volume of SAR data by effectively reducing the azimuth resolution, without loss of range resolution,

during times when end users are willing to accept lower azimuth resolution as the price of rapid access to SAR imagery. The data-reduction factor is selectable at a decimation factor,  $M$ , of 2, 4, 8, 16, or 32 so that users can trade



The **Prototype Circuit Board** measures 6 by 10 in. (15.2 by 25.4 cm). The AzPF integrated circuit mounted on the board measures only about 2.5 in. (=6.4 cm) square and consumes a power <1 W. The performance requirements are as follows: (1) Range resolution: No degradation in range resolution; (2) Azimuth resolution:  $1/M$  of original resolution for a single look; (3) Peak to side-lobe ratio (PSLR) after Hamming window: -25 dB; and (4) Integrated side-lobe ratio (ISLR) after Hamming window: -15 dB.

resolution against processing and transmission delays.

In principle, azimuth filtering could be performed in the frequency domain by use of fast-Fourier-transform processors. However, in the AzPF, azimuth filtering is performed in the time domain by use of finite-impulse-response filters. The reason for choosing the time-domain approach over the frequency-domain approach is that the time-domain approach demands less memory and a lower memory-access rate.

The AzPF operates on the raw digitized SAR data. The AzPF includes a digital in-phase/quadrature (I/Q) demodulator. In general, an I/Q demodulator effects a complex down-conversion of its input signal followed by low-pass filtering, which eliminates undesired sidebands. In the AzPF case, the I/Q demodulator takes offset video range echo data to the complex baseband domain, ensuring preservation of signal phase through the azimuth pre-filtering process. In general, in an SAR I/Q de-

modulator, the intermediate frequency ( $f_i$ ) is chosen to be a quarter of the range-sampling frequency and the pulse-repetition frequency ( $f_{PR}$ ) is chosen to be a multiple of  $f_i$ .

The AzPF also includes a polyphase spatial-domain pre-filter comprising four weighted integrate-and-dump filters with programmable decimation factors and overlapping phases. To prevent aliasing of signals, the bandwidth of the AzPF is made 80 percent of  $f_{PR}/M$ . The choice of four as the number of overlapping phases is justified by prior research in which it was shown that a filter of length  $4M$  can effect an acceptable transfer function.

The figure depicts prototype hardware comprising the AzPF and ancillary electronic circuits. The hardware was found to satisfy performance requirements in real-time tests at a sampling rate of 100 MHz.

*This work was done by Mimi Gudim, Tsan-Huei Cheng, Soren Madsen, Robert Johnson, Charles T-C Le, Mahta Moghadam, and Miguel Marina of Caltech for NASA's Jet Propulsion Laboratory. Further information is contained in a TSP (see page 1).*

NPO-30741



## ✚ Autonomous Navigation by a Mobile Robot

ROAMAN is a computer program for autonomous navigation of a mobile robot on a long (as much as hundreds of meters) traversal of terrain. Developed for use aboard a robotic vehicle (rover) exploring the surface of a remote planet, ROAMAN could also be adapted to similar use on terrestrial mobile robots. ROAMAN implements a combination of algorithms for (1) long-range path planning based on images acquired by mast-mounted, wide-baseline stereoscopic cameras, and (2) local path planning based on images acquired by body-mounted, narrow-baseline stereoscopic cameras. The long-range path-planning algorithm autonomously generates a series of waypoints that are passed to the local path-planning algorithm, which plans obstacle-avoiding legs between the waypoints. Both the long- and short-range algorithms use an occupancy-grid representation in computations to detect obstacles and plan paths. Maps that are maintained by the long- and short-range portions of the software are not shared because substantial localization errors can accumulate during any long traverse. ROAMAN is not guaranteed to generate an optimal shortest path, but does maintain the safety of the rover.

*This program was written by Terrance Huntsberger and Hrand Aghazarian of Caltech for NASA's Jet Propulsion Laboratory. Further information is contained in a TSP (see page 1).*

*This software is available for commercial licensing. Please contact Karina Edmonds of the California Institute of Technology at (818) 393-2827. Refer to NPO-30532.*

## ✚ Software Would Largely Automate Design of Kalman Filter

Embedded Navigation Filter Automatic Designer (ENFAD) is a computer program being developed to automate the most difficult tasks in designing embedded software to implement a Kalman filter in a navigation system. The most difficult tasks are selection of error states of the filter and tuning of filter parameters, which are time-consuming trial-and-error tasks that require expertise and rarely yield optimum results. An optimum selection of error states and filter parameters depends on navigation-sensor and vehicle characteris-

tics, and on filter processing time. ENFAD would include a simulation module that would incorporate all possible error states with respect to a given set of vehicle and sensor characteristics. The first of two iterative optimization loops would vary the selection of error states until the best filter performance was achieved in Monte Carlo simulations. For a fixed selection of error states, the second loop would vary the filter parameter values until an optimal performance value was obtained. Design constraints would be satisfied in the optimization loops. Users would supply vehicle and sensor test data that would be used to refine digital models in ENFAD. Filter processing time and filter accuracy would be computed by ENFAD.

*This program was written by Jason C. H. Chuang of Marshall Space Flight Center and William J. Negast, formerly of Gray Research, Inc. Further information is contained in a TSP (see page 1). MFS-31967-1*

## ✚ Predicting Flows of Rarefied Gases

DSMC Analysis Code (DAC) is a flexible, highly automated, easy-to-use computer program for predicting flows of rarefied gases — especially flows of upper-atmospheric, propulsion, and vented gases impinging on spacecraft surfaces. DAC implements the direct simulation Monte Carlo (DSMC) method, which is widely recognized as standard for simulating flows at densities so low that the continuum-based equations of computational fluid dynamics are invalid. DAC enables users to model complex surface shapes and boundary conditions quickly and easily. The discretization of a flow field into computational grids is automated, thereby relieving the user of a traditionally time-consuming task while ensuring (1) appropriate refinement of grids throughout the computational domain, (2) determination of optimal settings for temporal discretization and other simulation parameters, and (3) satisfaction of the fundamental constraints of the method. In so doing, DAC ensures an accurate and efficient simulation. In addition, DAC can utilize parallel processing to reduce computation time. The domain decomposition needed for parallel processing is completely automated, and the software employs a dynamic load-balancing mechanism to ensure optimal parallel efficiency throughout the simulation.

*This work was done by Gerald J. LeBeau of Johnson Space Center and Richard G. Wilmoth of Langley Research Center. For further information, contact the Johnson Innovative Partnerships Office at (281) 483-3809. MSC-23445*

## ✚ Centralized Planning for Multiple Exploratory Robots

A computer program automatically generates plans for a group of robotic vehicles (rovers) engaged in geological exploration of terrain. The program rapidly generates multiple command sequences that can be executed simultaneously by the rovers. Starting from a set of high-level goals, the program creates a sequence of commands for each rover while respecting hardware constraints and limitations on resources of each rover and of hardware (e.g., a radio communication terminal) shared by all the rovers. First, a separate model of each rover is loaded into a centralized planning subprogram. The centralized planning software uses the models of the rovers plus an iterative repair algorithm to resolve conflicts posed by demands for resources and by constraints associated with the all the rovers and the shared hardware. During repair, heuristics are used to make planning decisions that will result in solutions that will be better and will be found faster than would otherwise be possible. In particular, techniques from prior solutions of the multiple-traveling-salesmen problem are used as heuristics to generate plans in which the paths taken by the rovers to assigned scientific targets are shorter than they would otherwise be.

*This program was written by Tara Estlin, Gregg Rabideau, Steve Chien, and Anthony Barrett of Caltech for NASA's Jet Propulsion Laboratory. Further information is contained in a TSP (see page 1).*

*This software is available for commercial licensing. Please contact Karina Edmonds of the California Institute of Technology at (818) 393-2827. Refer to NPO-35192.*

## ✚ Electronic Router

Electronic Router (E-Router) is an application program for routing documents among the cognizant individuals in a government agency or other organization. E-Router supplants a prior

system in which paper documents were routed physically in packages by use of paper slips, packages could be lost, routing times were unacceptably long, tracking of packages was difficult, and there was a need for much photocopying. E-Router enables a user to create a digital package to be routed. Input accepted by E-Router includes the title of the package, the person(s) to whom the package is to be routed, attached files, and comments to reviewers. Elec-

tronic mail is used to notify reviewers of needed actions. The creator of the package can, at any time, see the status of the package in the routing structure. At the end of the routing process, E-Router keeps a record of the package and of approvals and/or concurrences of the reviewers. There are commercial programs that perform the general functions of E-Router, but they are more complicated. E-Router is Web-based, easy to use, and does not re-

quire the installation or use of client software.

*This program was written by Jason Crusan of Indyne, Inc., for **Glenn Research Center**. For further information, contact Jason Crusan at [jason.c.crusan@grc.nasa.gov](mailto:jason.c.crusan@grc.nasa.gov).*

*Inquiries concerning rights for the commercial use of this invention should be addressed to NASA Glenn Research Center, Innovative Partnerships Office, Attn: Steve Fedor, Mail Stop 4-8, 21000 Brookpark Road, Cleveland, Ohio 44135. Refer to LEW-17497-1*

## ⊕ Piezo-Operated Shutter Mechanism Moves 1.5 cm

**This shutter is designed for use as part of an atomic clock.**

*NASA's Jet Propulsion Laboratory, Pasadena, California*

The figure shows parts of a shutter mechanism designed to satisfy a number of requirements specific to its original intended application as a component of an atomic clock to be flown in outer space. The mechanism may also be suitable for use in laboratory and industrial vacuum systems on Earth for which there are similar requirements. The requirements include the following:

- To alternately close, then open, a 1.5-cm-diameter optical aperture twice per second, with a stroke time of no more than 15 ms, during a total operational lifetime of at least a year;
- To attenuate light by a factor of at least  $10^{12}$  when in the closed position;
- To generate little or no magnetic field;
- To be capable of withstanding bakeout at a temperature of 200 °C to minimize outgassing during subsequent operation in an ultrahigh vacuum; and
- To fit within a diameter of 12 in. ( $\approx 305$  mm) — a size limit dictated by the size of an associated magnetic shield.

The light-attenuation requirement is satisfied by use of overlapping shutter blades. The closure of the aperture involves, among other things, insertion of a single shutter blade between a pair of shutter blades. The requirement to minimize the magnetic field is satisfied by use of piezoelectric actuators. Because piezoelectric actuators cannot withstand bakeout, they must be mounted outside the vacuum chamber, and, hence, motion must be transmitted from the actuators to the shutter levers via a vacuum-chamber-wall diaphragm.

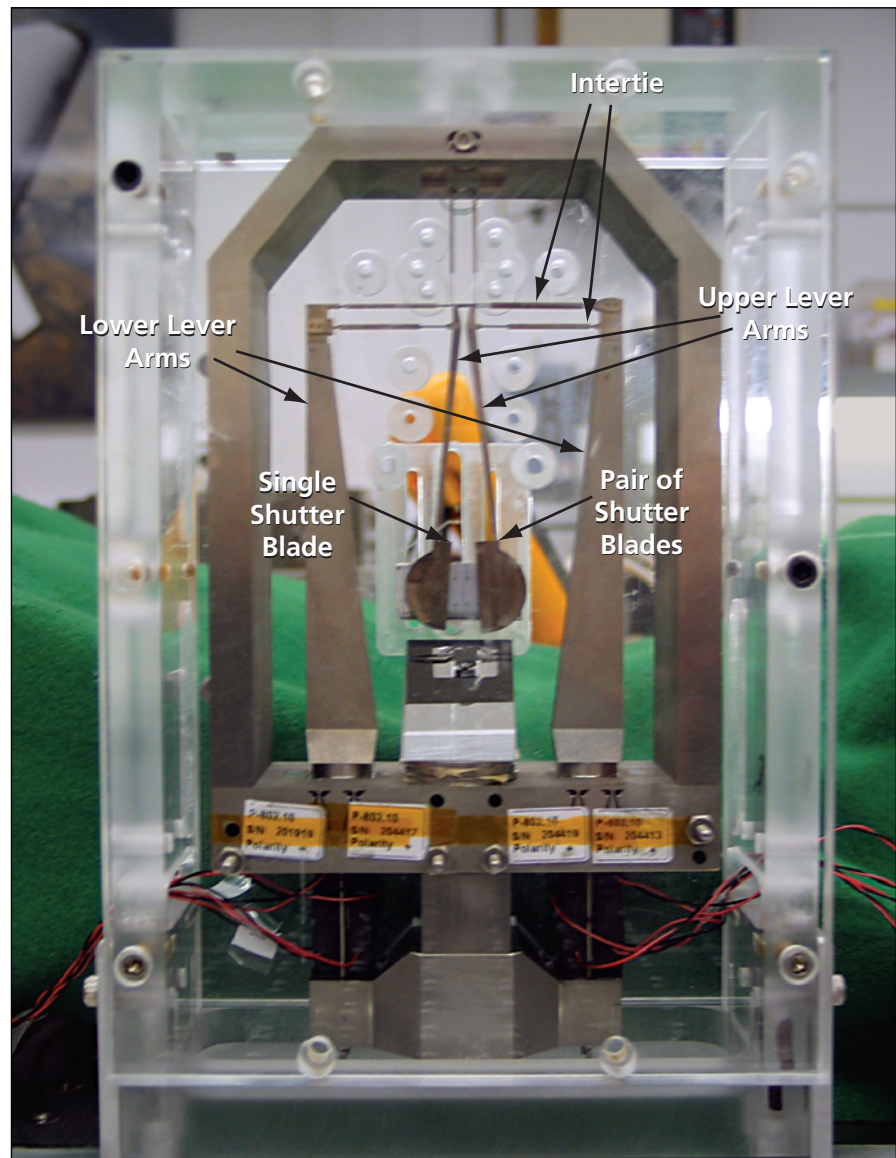
The mechanism inside the vacuum chamber must be fabricated in one piece to eliminate pockets from which trapped gas could later escape, ruining the ultrahigh vacuum. The smallness of the displacement produced by the piezoelectric actuators gives rise to a need for mechanical amplification of the stroke by a factor of about 700. The requirement for mechanical amplification is satisfied by use of two pairs of lever arms that are mirror images of each other. The requirement for one-piece construction dictates the use of flexures, instead of bearings, to accom-

modate the pivoting of the levers.

The piezoelectric actuators, which are also mirror images of each other, are mounted outside the vacuum system (underneath the frame shown in the figure), where they are connected to the lower ends of the lower levers. The upper ends of the lower levers are coupled to the upper ends of the upper levers through a cross-coupled flexing inertia, which is

also connected to supports to fix the pivot locations and to hold the diaphragm against atmospheric pressure. The shutter blades are mounted on the lower ends of the upper levers.

*This work was done by Robert Glaser and Robert Bamford of Caltech for NASA's Jet Propulsion Laboratory. Further information is contained in a TSP (see page 1). NPO-40394*



The **Shutter Is Open** in this view. To close the shutter, the levers are pivoted such that the single shutter blade on the left side and the pair of shutter blades on the right side are both brought to the center, so that the blades overlap to block the central aperture.

## Two SMA-Actuated Miniature Mechanisms

These mechanisms represent two different approaches to latch/release operation.

Goddard Space Flight Center, Greenbelt, Maryland

The figures depict two miniature mechanisms actuated by strips made of shape-memory alloy (SMA). A typical SMA is a nickel-titanium alloy known by the trade name "Flexinol" or "Nitinol." In

preparation for a typical application, a suitably sized and shaped piece of an SMA is deformed by a predetermined amount at the lower of two operating temperatures, then mounted in a mecha-

nism. When stroking of the mechanism in one direction is desired, the piece of SMA is heated above a transition temperature to make it return to the "remembered" undeformed state. When stroking

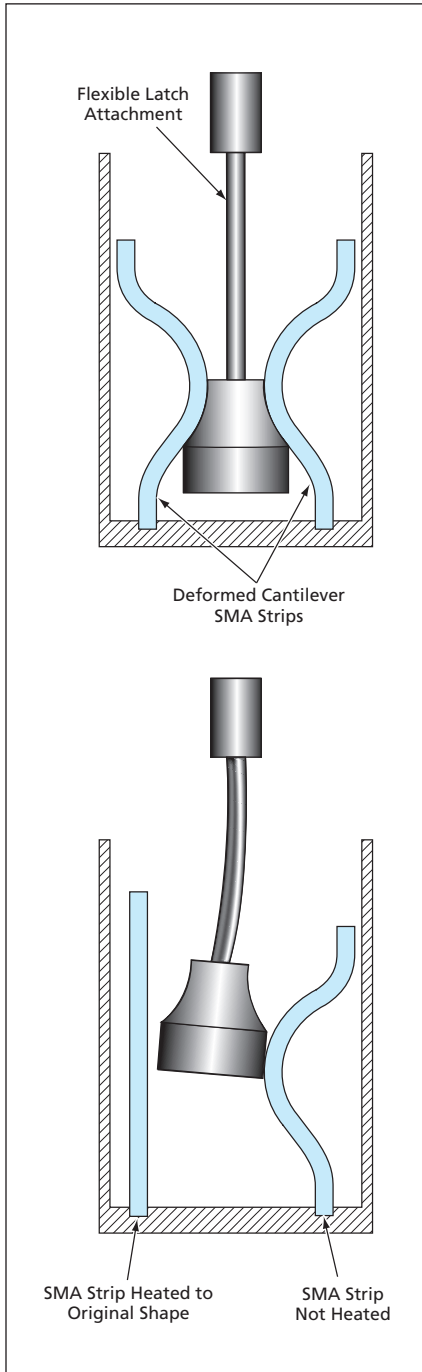


Figure 1. Two Bent SMA Strips act as two halves of a clamp that retains the knob. Both SMA strips are supposed to straighten when heated to release the knob. However, even if only one SMA strip straightens, the knob is released.

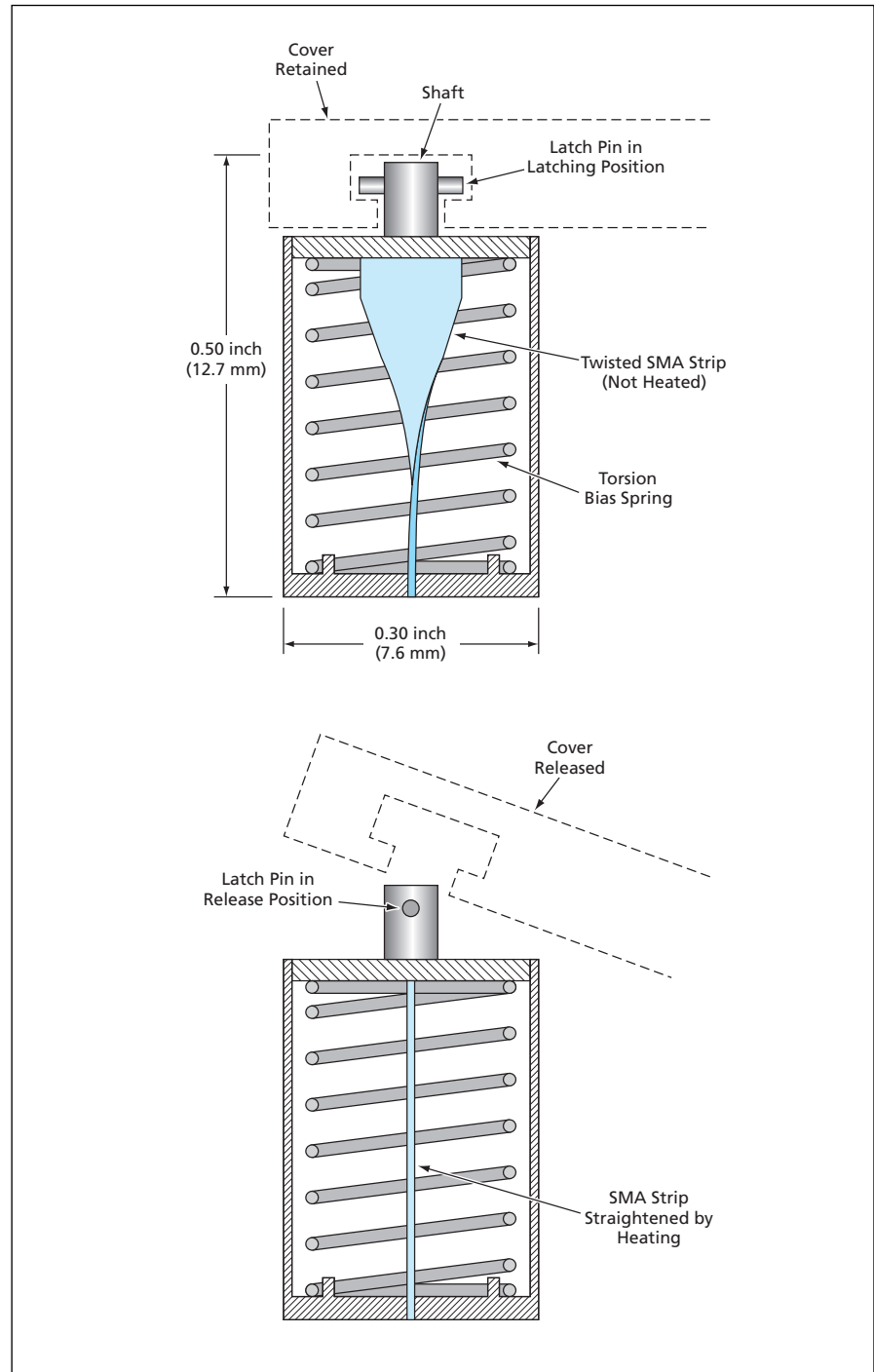


Figure 2. A Torsion Bias Spring and a Twisted SMA Strip cause the shaft holding the latch pin to rotate through a 90° angle to a release position when the SMA strip is heated above its transition temperature.

of the mechanism in the opposite direction is desired, the SMA is cooled below the transition temperature to make it return to the deformed state.

Also, the SMA alloy chosen for a specific application is one that has a transition temperature somewhat above the ambient temperature, so that stroking in one direction or the opposite direction can be achieved by heating the SMA, or refraining from heating the SMA, respectively, above the transition temperature. In the present mechanisms as in typical other SMA mechanisms, the heating is effected by electric currents applied via electrical contacts at the ends of the SMA strips.

The purpose served by the mechanism of Figure 1 is to lock or release a

flexible latch attachment. In preparation for use in this mechanism, two initially straight SMA strips are deformed into curved springs that, when mounted in the mechanism at ambient temperature, clamp the knob at the lower end of the flexible latch attachment. When heated above their transition temperature by an electric current, the SMA strips return to their original straight configuration, thereby releasing the knob. This mechanism is redundant in the sense that as long as at least one of the two SMA strips straightens when commanded to do so, the knob is released.

The mechanism of Figure 2 is suited to any of a variety of applications in

which there are requirements for a small mechanism that affords low-torque rotary actuation through a finite angular range. As shown here, the mechanism is used to rotate a cover-latch pin to a release position. In this case, a straight and flat SMA strip is torsionally deformed to a twist angle of about 90° by use of a torsion bias spring. When the SMA strip is heated, it rotates to its original straight and flat condition.

*This work was done by Cliff E. Willey of Johns Hopkins University Applied Physics Laboratory for **Goddard Space Flight Center**. For further information contact Nona Cheeks at [Nona.K.Cheeks.1@gsfc.nasa.gov](mailto:Nona.K.Cheeks.1@gsfc.nasa.gov) GSC-14705-1*



## Vortobots

Vortex-generating microscopic robots would move in swarms.

NASA's Jet Propulsion Laboratory, Pasadena, California

The term "vortobots" denotes proposed swimming robots that would have dimensions as small as micrometers or even nanometers and that would move in swarms through fluids by generating and exploiting vortices in a cooperative manner. Vortobots were conceived as means of exploring confined or otherwise inaccessible fluid environments: they are expected to be especially attractive for biomedical uses like examining

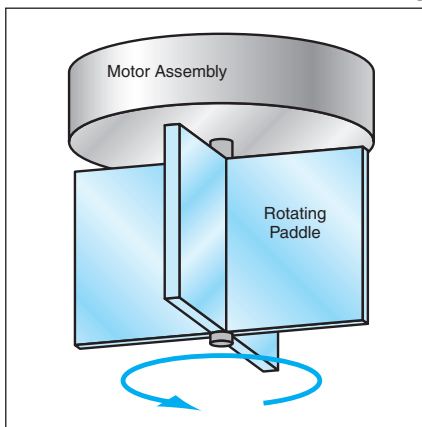


Figure 1. A Spinning Paddle on a floating micro-robot would generate a vortex in the surrounding fluid.

the interiors of blood vessels.

The main advantage of the vortobot concept, relative to other concepts for swimming microscopic robots, is that the mechanisms for locomotion would be relatively simple and, therefore, could be miniaturized more easily. For example, only a simple spinning paddle would be required to generate a vortex around a vortobot (see Figure 1). The difficulty is that a smart swarming and cooperative control algorithm would be necessary for purposeful locomotion. This necessity arises because, as a consequence of basic principles of vortex dynamics, an isolated single vortex cannot move by itself because its induced flow at the center is zero; however, a vortex can move other vortices by the induced flow. By cleverly adjusting the strength and sign of each member in a group of vortices, the group can achieve net translational motion in the preferred direction through cooperation.

Figure 2 presents two simple examples that serve to illustrate the principle of cooperative motion of vortobots. For the sake of simplicity, these examples are based on an idealized two-dimensional potential flow of an inviscid, incompress-

ible liquid. The example of the upper part of the figure is of two vortices of equal magnitude and opposite sign. The centers of the vortices would move along parallel paths. The example of the lower part of the figure is of two vortices of the same magnitude and sign. In this case, both vortices would move in a circle in diametrically opposite positions. More complex motions can be obtained by introducing more vortices (or pairs of vortices) and choosing different vortex strengths and orientations.

Alternatively or in addition to what has been described thus far, vortobots could be equipped with simple oscillating source/sink mechanisms. Like a vortex, an oscillating source/sink generated by a single floating object would result in little or no net translational motion, whereas multiple oscillating source/sinks could produce net translational motion.

Of course, it would be necessary to control the vortobots in a swarm to obtain the cooperative action needed for locomotion. Both global and local control algorithms are under investigation. A global algorithm would be based on knowledge of the position of every vortobot and would strive to control the overall motion of the swarm. A local algorithm would not depend on explicit knowledge of the positions of the vortobots, but rather the local influence of nearby vortobots. This type of algorithm would be implemented independently in each vortobot, and would be formulated so that the combined effect of the independent actions of the vortobots would be the desired collective behavior. For the purpose of a local control algorithm, vortobots could communicate with neighboring vortobots indirectly through such sensed fluid parameters as shear, pressure, and concentration. For longer-range communication (which would be necessary for a global control algorithm), sound waves could be used.

*This work was done by Han Park and Flavio Noca of Caltech and Petros Koumoutsakos of ETH Zurich, Switzerland, for NASA's Jet Propulsion Laboratory. Further information is contained in a TSP (see page 1). NPO-21188*

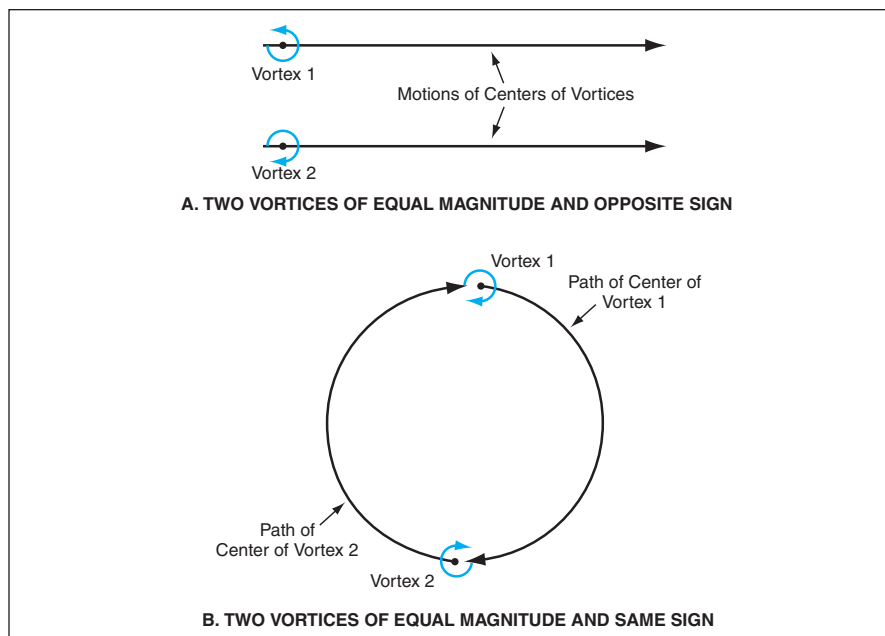


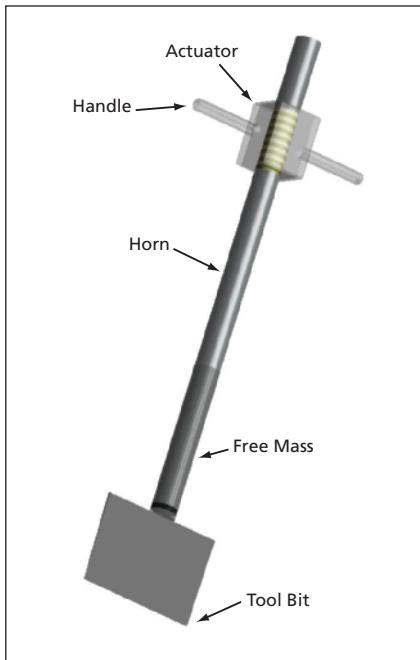
Figure 2. Two Vortices of Equal Magnitude would move along parallel lines or around a common center, depending on whether they were of opposite sign or the same sign, respectively.

## Ultrasonic/Sonic Jackhammer

Advantages include low noise, low vibration, and low average power demand.

NASA's Jet Propulsion Laboratory, Pasadena, California

An ultrasonic/sonic jackhammer (USJ) is the latest in a series of related devices, the first of which were reported in "Ultrasonic/Sonic Drill/Corers With Integrated Sensors" (NPO-20856), *NASA Tech Briefs*, Vol. 25, No. 1 (January 2003), page 38. Each of these devices cuts into a brittle material by means of hammering and chiseling actions of a tool bit excited with a combination of ultrasonic and sonic vibrations. A small-scale prototype of the USJ has been demonstrated. A fully developed, full-scale version of the USJ would be used for cutting through concrete, rocks, hard asphalt, and other materials to which conventional pneumatic jackhammers are applied, but



The **Ultrasonic/Sonic Jackhammer** is driven electrically instead of pneumatically. It offers several advantages over a conventional pneumatic jackhammer.

the USJ would offer several advantages over conventional pneumatic jackhammers, as discussed below.

In the USJ (see figure) as in the previously reported ultrasonic/sonic drill/corers (USDCs) and related devices, the actuator assembly includes a piezoelectric stack and a horn for mechanical amplification of the piezoelectric displacement. A cylindrical shank of a chisel-shaped tool bit is mounted on the lower end of the horn. A bobbin-like cylindrical mass is free to move axially through a limited range between the lower end of the horn and the upper end of the blade portion of the tool bit. The sharp edge of the bit is placed in contact with the rock or other hard material to be cut. Unlike a pneumatic jackhammer, the USJ need not be heavy because its principle of operation does not require a large contact force.

The piezoelectric stack is electrically driven at its resonance frequency, and a bolt holds the stack in compression to prevent fracture during operation. The free mass bounces between hard stops at the limits of its range of motion at a sonic frequency. The impacts of the free mass on the hard stops create stress pulses that propagate along the horn, to and through the tool bit, to the tool-bit/rock interface. The rock becomes fractured when its ultimate strain is exceeded.

A conventional pneumatic jackhammer generates enormous amounts of noise, along with severe vibrations that propagate back into the operator's body and that are so strong as to sometimes injure the operator. Every object encountered by the tool bit is damaged. This indiscriminate cutting action is particularly disadvantageous in

situations in which there is a need to cut through concrete or asphalt without damaging such embedded objects as pipes, cables, and reinforcing steel bars.

In contrast, even a full-scale USJ would generate much less noise and much less back-propagating vibration. The full-scale USJ would also demand less average power. Moreover, on the basis of experience with the USDCs, it is expected that such relatively flexible materials as wood, plastics, metals, and human tissues will not be damaged by brief contact with the tool bit of the operating USJ. Yet another advantage is that like a USDC as described in the noted prior *NASA Tech Briefs* article, the USJ could be instrumented with mechanical-impedance sensors that could be used to obtain feedback to optimize the electrical excitation for cutting and/or to utilize the vibrations to probe the hard material in the vicinity of the tool bit.

*This work was done by Yoseph Bar-Cohen and Stewart Sherrit of Caltech and Jack Herz of CTC for NASA's Jet Propulsion Laboratory. Further information is contained in a TSP (see page 1).*

*In accordance with Public Law 96-517, the contractor has elected to retain title to this invention. Inquiries concerning rights for its commercial use should be addressed to:*

*Innovative Technology Assets Management  
JPL*

*Mail Stop 202-233  
4800 Oak Grove Drive  
Pasadena, CA 91109-8099  
(818) 354-2240*

*E-mail: iaoffice@jpl.nasa.gov*

*Refer to NPO-40771, volume and number of this NASA Tech Briefs issue, and the page number.*



## Removing Pathogens Using Nano-Ceramic-Fiber Filters

**Filters remove greater than 99.9999 percent of viruses and bacteria from wastewater.**

*Lyndon B. Johnson Space Center, Houston, Texas*

A nano-aluminum-oxide fiber of only 2 nanometers in diameter was used to develop a ceramic-fiber filter. The fibers are electropositive and, when formulated into a filter material (NanoCeram<sup>®</sup>), would attract electronegative particles such as bacteria and viruses. The ability to detect and then remove viruses as well as bacteria is of concern in space cabins since they may be carried onboard by space crews. Moreover, an improved filter was desired that would polish the effluent from condensed moisture and wastewater, producing potable drinking water. A laboratory-size filter was developed that was capable of removing greater than 99.9999 percent of bacteria and virus. Such a removal was achieved at flow rates hundreds of times greater than those through ultraporous membranes that remove particles by sieving. Because the pore size of the new filter was rather large as compared to ultraporous membranes, it was found to be more resistant to clogging.

Additionally, a full-size cartridge is being developed that is capable of serving a full space crew. During this ongoing effort, research demonstrated that the filter media was a very efficient adsorbent for DNA (deoxyribonucleic acid), RNA (ribonucleic acid), and endotoxins. Since the adsorption is based on the charge of the macromolecules, there is also a potential for separating proteins and other particulates on the basis of their charge differences. The separation of specific proteins is a major new thrust of biotechnology.

The principal application of NanoCeram<sup>®</sup> filters is based on their ability to remove viruses from water. The removal of more than 99.9999 percent of viruses was achieved by a NanoCeram<sup>®</sup> polishing filter added to the effluent of an existing filtration device. NanoCeram<sup>®</sup> is commercially available in laboratory-size filter discs and in the form of a syringe filter. The unique characteristic of the filter can be demonstrated by its ability to remove particulate dyes such as

Metanyl yellow. Its particle size is only 2 nanometers, about the size of a DNA molecule, yet the NanoCeram<sup>®</sup> syringe filter is capable of retaining the dyes as the fluid is passed through the syringe, without much backpressure. Endotoxins, which are contaminants that are part of the residue of destroyed bacteria, can cause toxic shock and are therefore of major concern in pharmaceutical products. The NanoCeram<sup>®</sup> syringe filter is capable of removing greater than 99.96 percent of the endotoxins.

*This work was done by Frederick Tepper and Leonid Kaledin of Argonide Corp. for Johnson Space Center.*

*In accordance with Public Law 96-517, the contractor has elected to retain title to this invention. Inquiries concerning rights for its commercial use should be addressed to:*

*Argonide Corporation  
291 Power Court  
Sanford, FL 32771*

*Refer to MSC-23478, volume and number of this NASA Tech Briefs issue, and the page number.*

## Satellite-Derived Management Zones

**Precision agriculture can be practiced at low cost.**

*Stennis Space Center, Mississippi*

The term "satellite-derived management zones" (SAMZ) denotes agricultural management zones that are subdivisions of large fields and that are derived from images of the fields acquired by instruments aboard Earth-orbiting satellites during approximately the past 15 years. "SAMZ" also denotes the methodology and the software that implements the methodology for creating such zones. The SAMZ approach is one of several products of continuing efforts to realize a concept of precision agriculture, which involves optimal variations in seeding, in application of chemicals, and in irrigation, plus decisions to farm or not to farm certain portions of fields, all in an effort to maximize profitability in view of spatial

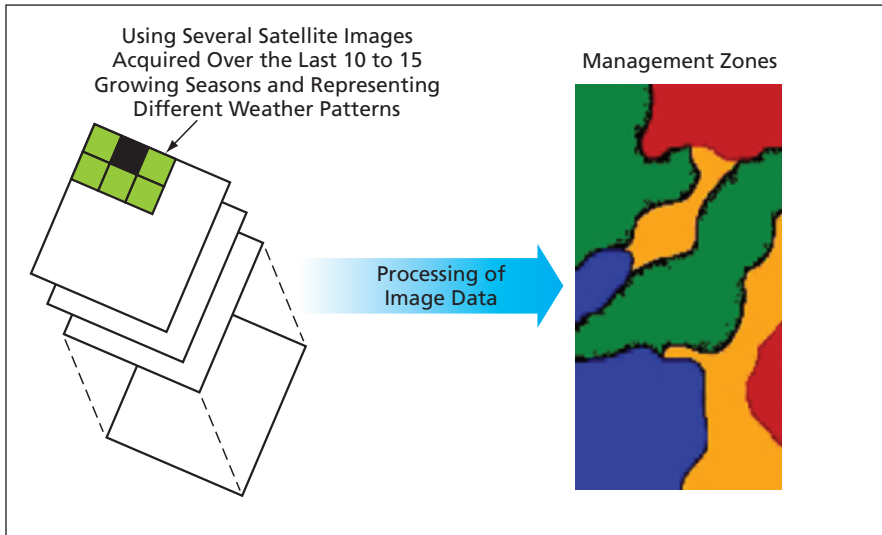
and temporal variations in the growth and health of crops, and in the chemical and physical conditions of soils.

As used here, "management zone" signifies, more precisely, a subdivision of a field within which the crop-production behavior is regarded as homogeneous. From the perspective of precision agriculture, management zones are the smallest subdivisions between which the seeding, application of chemicals, and other management parameters are to be varied.

In the SAMZ approach, the main sources of data are the archives of satellite imagery that have been collected over the years for diverse purposes. One of the main advantages afforded by the SAMZ approach is that the data in these

archives can be reused for purposes of precision agriculture at low cost. *De facto*, these archives contain information on all sources of variability within a field, including weather, crop types, crop management, soil types, and water drainage patterns.

The SAMZ methodology involves the establishment of a Web-based interface based on an algorithm that generates management zones automatically and quickly from archival satellite image data in response to requests from farmers. A farmer can make a request by either uploading data describing a field boundary to the Web site or else drawing the boundary on a reference image. Hence, a farmer can start to engage in precision farming shortly after gaining



**Multiple Satellite Images of a Field** are analyzed to identify zones for which different precision-agriculture treatments are needed.

access to the Web site, without the need for incurring the high costs of conventional precision-agriculture data-collection practices that include collecting soil samples, mapping electrical con-

ductivity of soil, and compiling multi-year crop-yield data.

Given the boundary of a field, a SAMZ server computes the zones within the field in a three-stage process. In the first

stage, a vector-valued image of the field is constructed by assembling, from the archives, the equivalent of a stack of the available images of the field (see figure). In the second stage, the vector-valued image is analyzed by use of a wavelet transform that detects spatial variations considered significant for precision farming while suppressing small-scale heterogeneities that are regarded as insignificant. In the third stage, a segmentation algorithm assembles the zones from smaller regions that have been identified in the wavelet analysis.

*This work was done by Damien Lepoutre and Laurent Layrol of GEOSYS, Inc., for Stennis Space Center.*

*In accordance with Public Law 96-517, the contractor has elected to retain title to this invention. Inquiries concerning rights for its commercial use should be addressed to:*

*GEOSYS, Inc.*

*3030 Harbor Lane*

*Plymouth, MN 55447*

*Refer to SSC-00186, volume and number of this NASA Tech Briefs issue, and the page number.*



## Digital Equivalent Data System for XRF Labeling of Objects

### Conventions for XRF labels and converting XRF spectra to alphanumeric data leads to new identification method.

*Marshall Space Flight Center, Alabama*

A digital equivalent data system (DEDS) is a system for identifying objects by means of the x-ray fluorescence (XRF) spectra of labeling elements that are encased in or deposited on the objects. As such, a DEDS is a revolutionary new major subsystem of an XRF system. A DEDS embodies the means for converting the spectral data output of an XRF scanner to an ASCII alphanumeric or bar-code label that can be used to identify (or verify the assumed or apparent identity of) an XRF-scanned object.

A typical XRF spectrum of interest contains peaks at photon energies associated with specific elements on the Peri-

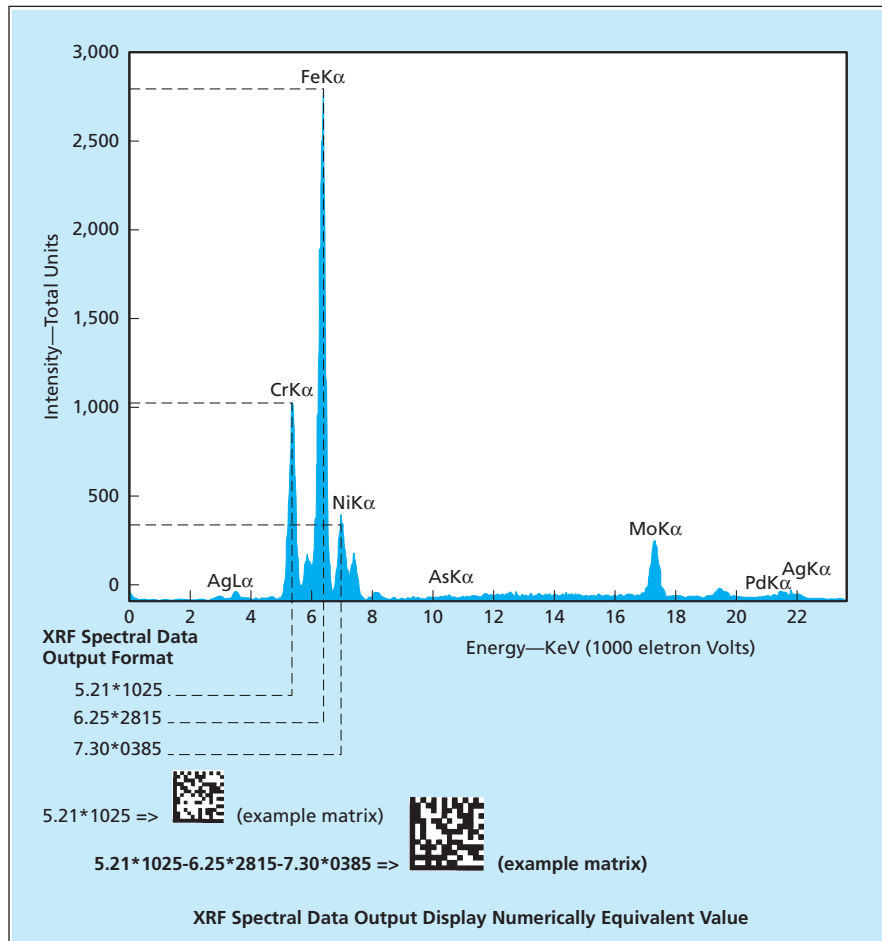
odic Table (see figure). The height of each spectral peak above the local background spectral intensity is proportional to the relative abundance of the corresponding element. Alphanumeric values are assigned to the relative abundances of the elements. Hence, if an object contained labeling elements in suitably chosen proportions, an alphanumeric representation of the object could be extracted from its XRF spectrum. The mixture of labeling elements and for reading the XRF spectrum would be compatible with one of the labeling conventions now used for bar codes and binary matrix patterns (essentially, two-di-

mensional bar codes that resemble checkerboards). A further benefit of such compatibility is that it would enable the conversion of the XRF spectral output to a bar or matrix-coded label, if needed. In short, a process previously used only for material composition analysis has been reapplied to the world of identification. This new level of verification is now being used for "authentication."

The DEDS as described thus far would be used to process XRF spectral data output only. In one of several alternatives, an object could be labeled with both a conventional bar or matrix code and an XRF tag, so that the XRF tag could be used to provide redundant, additional, or confirmatory information. In that case, the DEDS would analyze the XRF tag and convert the readings to alphanumeric data in a recognized format. In yet another alternative, the XRF scanner would be used to acquire an XRF spectrum of not only the XRF tag but also the substrate material surrounding the tag. In that case, the spectral data output from the substrate would constitute an additional set of data that could be combined with the XRF label data and the bar-code or matrix readout to obtain an alphanumeric label unique to the labeled object or to the class that it represents.

Authentication is the natural evolution of the identification process as security technologies are combined with it. The XRF DEDS provides a unique set of methods to determine if an object is genuine. The respective sets of information cannot be duplicated and answers the question "is that the original object."

Authentication using XRF DEDS is expected to have no negative impact on existing networks as its conversion is in ASCII format, and convertible to bar code or other symbology formats. In fact it is expected to simply "fit in" with other members of the identification technology family. It is intended as a process to eliminate counterfeits and knock-offs, enabling the routine data collection in the downstream process



The Coordinates of Each Peak in an XRF Spectrum of a label would contribute information on the contents of the label: The horizontal coordinate would indicate a photon energy and, hence, the identity of an element; the vertical coordinate would indicate the spectral intensity and, hence, the abundance of the element.

using bar codes and matrix codes to be much more secure. Finally, it is expected to find its way into the courtroom, having the unique insight as to which object is genuine and which is not. Authentication using XRF DEDS may well be the next-generation expert witness in product liability cases.

*This work was done by Harry F. Schramm of Marshall Space Flight Center and Bruce Kaiser of Keymaster Technologies, Inc. For further information, contact Sammy Nabors, MSFC Commercialization Assistance Lead, at sammy.a.nabors@nasa.gov.*

*In accordance with Public Law 96-517, the contractor has elected to retain title to this in-*

*vention. Inquiries concerning rights for its commercial use should be addressed to:*

*Keymaster Technologies, Inc.  
415 N. Quay Street, Suite 1  
Kennewick, WA 99336*

*Refer to MFS-31886, volume and number of this NASA Tech Briefs issue, and the page number.*

## Identifying Objects via Encased X-Ray-Fluorescent Materials — the Bar Code Inside

**XRF spectra would be used as labels, similarly to bar codes, inside a product.**

*Marshall Space Flight Center, Alabama*

Systems for identifying objects by means of x-ray fluorescence (XRF) of encased labeling elements have been developed. The XRF spectra of objects so labeled would be analogous to the external bar code labels now used to track objects in everyday commerce. In conjunction with computer-based tracking systems, databases, and labeling conventions, the XRF labels could be used in essentially the same manner as that of bar codes to track inventories and to record and process commercial transactions. In addition, as summarized briefly below, embedded XRF labels could be used to verify the authenticity of products, thereby helping to deter counterfeiting and fraud.

A system, as described above, is called an “encased core product identification and authentication system” (ECPIAS).

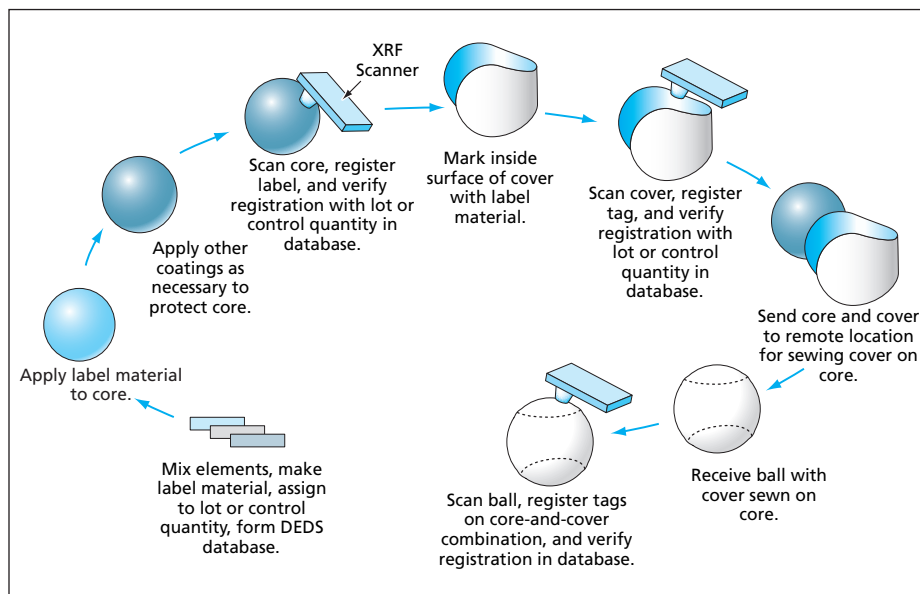
The ECPIAS concept is a modified version of that of a related recently initiated commercial development of handheld XRF spectral scanners that would identify alloys or detect labeling elements deposited on the surfaces of objects. In contrast, an ECPIAS would utilize labeling elements encased within the objects of interest.

The basic ECPIAS concept is best illustrated by means of an example of one of several potential applications: labeling of cultured pearls by labeling the seed particles implanted in oysters to grow the pearls. Each pearl farmer would be assigned a unique mixture of labeling elements that could be distinguished from the corresponding mixtures of other farmers. The mixture would be either incorporated into or applied to the surfaces of the seed prior to implantation in

the oyster. If necessary, the labeled seed would be further coated to make it non-toxic to the oyster. After implantation, the growth of layers of mother of pearl on the seed would encase the XRF labels, making these labels integral, permanent parts of the pearls that could not be removed without destroying the pearls themselves. The XRF labels would be read by use of XRF scanners, the spectral data outputs of which would be converted to alphanumeric data in a digital equivalent data system (DEDS), which is the subject of the previous article. These alphanumeric data would be used to track the pearls through all stages of commerce, from the farmer to the retail customer.

In another potential application (see figure), an ECPIAS would be used to track softballs. Softball cores and covers are typically manufactured in the United States and shipped offshore where the covers are sewn on. At present, in order to verify the origin of a shipment of assembled softballs returning to the United States, it is necessary to take some balls as samples, cut their covers off, and examine their cores. In contrast, the ECPIAS would make it possible to verify the origin of the balls quickly and nondestructively. The ECPIAS concept could also be applied to other products in which XRF labels could be permanently encased. Examples include balls used in high-profile sports, tires, printed-circuit components, layered clothing items (e.g., shoes), and critical aircraft components.

The ECPIAS is a “next logical step” technology that gives an OEM a new safeguard for product liability. With the bar code inside the part or even mixed with the material of the



**Softball Cores and Covers Would Be Labeled** by mixtures of elements having unique XRF spectra. The balls would be tracked through the stages of manufacture and transport by using the spectra to verify their identities.

part, authentication can be attained with a simple scan. For those who have ever tried to put a barcode inside a pearl, ECPIAS may sound like a good alternative.

*This work was done by Harry F. Schramm of Marshall Space Flight Center, and*

*Bruce Kaiser of Keymaster Technologies, Inc. For further information, contact Sammy Nabors, MSFC Commercialization Assistance Lead, at sammy.nabors@msfc.nasa.gov.*

*In accordance with Public Law 96-517, the contractor has elected to retain title to this invention. Inquiries concerning rights for its*

*commercial use should be addressed to: Keymaster Technologies, Inc. 415 N. Quay Street, Suite 1 Kennewick, WA 99336*

*Refer to MFS-31890, volume and number of this NASA Tech Briefs issue, and the page number.*

## Vacuum Attachment for XRF Scanner

**A greater range of elements could be analyzed.**

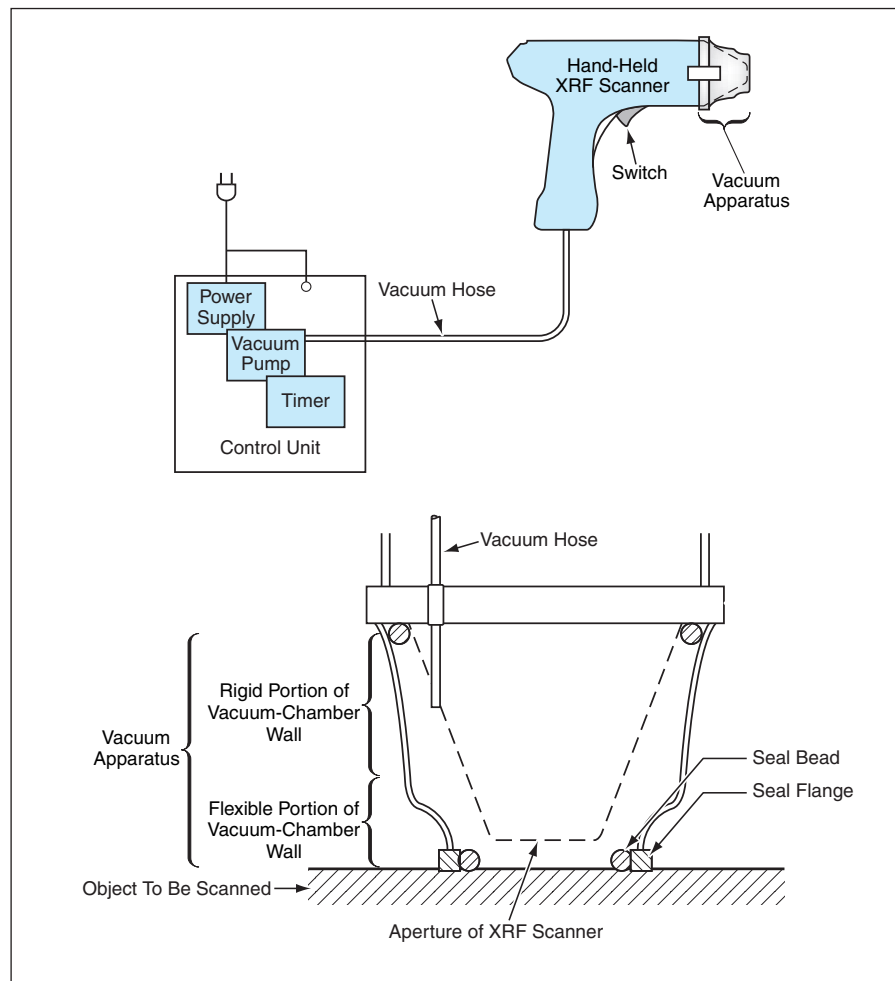
*Marshall Space Flight Center, Alabama*

Vacuum apparatuses have been developed for increasing the range of elements that can be identified by use of x-ray fluorescent (XRF) scanners of the type mentioned in the two immediately preceding articles. As a consequence of the underlying physical principles, in the presence of air, such an XRF scanner is limited to analysis of chlorine and elements of greater atomic number. When the XRF scanner is operated in a vacuum, it extends the range of analysis to lower atomic numbers — even as far as aluminum and sodium. Hence, more elements will be available for use in XRF labeling of objects as discussed in the two preceding articles.

The added benefits of the extended capabilities also have other uses for NASA. Detection of elements of low atomic number is of high interest to the aerospace community. High-strength aluminum alloys will be easily analyzed for composition. Silicon, a major contaminant in certain processes, will be detectable before the process is begun, possibly eliminating weld or adhesion problems. Exotic alloys will be evaluated for composition prior to being placed in service where lives depend on them. And in the less glamorous applications, such as bolts and fasteners, substandard products and counterfeit items will be evaluated at the receiving function and never allowed to enter the operation.

Both hand-held and tabletop XRF portable scanners have been developed. The vacuum apparatus is compact and lightweight and does not detract from the portability of either XRF scanner. It is attached to and detached from the aperture end of either XRF scanner.

The upper part of the figure schematically depicts the hand-held XRF scanner. The XRF scanner and vacuum apparatus would be connected to a portable (belt-mounted) control unit that would contain



A Compact Vacuum Apparatus attached to the aperture end of a hand-held XRF scanner would enable vacuum XRF analysis without the need to mount the entire XRF scanner in a vacuum chamber.

a power supply and a vacuum pump. The lower part of the figure is a simplified, enlarged cross-sectional view of a vacuum apparatus attached to the aperture end of the XRF scanner. The side wall of the vacuum apparatus would include a flexible portion that would support a seal flange and seal bead, which would be pressed against an object to be scanned to form an air-tight seal. While holding the seal and

pressing the aperture of the XRF scanner against the object to be scanned, the operator would press a switch, thereby starting the process. The switch would turn on the pump and keep it on for as long as needed to maintain the vacuum needed for the XRF scan.

The vacuum enhanced version of the hand-held XRF, already in use in the shuttle program, takes the chemistry lab

to the shop floor, something that was not practical to do before with large products such as external tanks, space shuttle main engines, and solid rocket boosters. From label scanning to material analysis, the vacuum enhanced XRF is a welcome addition to the NASA toolbox of capabilities.

*This work was done by Harry F. Schramm of Marshall Space Flight Center and Bruce Kaiser of Keymaster Technologies, Inc. For further information, contact Sammy Nabors, MSFC Commercialization Assistance Lead, at sammy.nabors@msfc.nasa.gov.*

*In accordance with Public Law 96-517, the contractor has elected to retain title to this in-*

*vention. Inquiries concerning rights for its commercial use should be addressed to:*

*Keymaster Technologies, Inc.  
415 N. Quay Street, Suite 1  
Kennewick, WA 99336*

*Refer to MFS-31898, volume and number of this NASA Tech Briefs issue, and the page number.*

## Simultaneous Conoscopic Holography and Raman Spectroscopy

**Both the topography and the chemistry of surfaces would be mapped.**

*NASA's Jet Propulsion Laboratory, Pasadena, California*

A new instrument was developed for chemical characterization of surfaces that combines the analytical power of Raman spectroscopy with the three-dimensional topographic information provided by conoscopic holography. The figure schematically depicts the proposed hybrid instrument. The output of the conoscopic holographic portion of the instrument is a topographical map of the surface; the output of the Raman portion of the instrument is hyperspectral Raman data, from which the chemical and/or biological composition of the surface would be deduced. By virtue of the basic principles of design and operation of the instrument, the hyperspectral image data would be inherently spatially registered with the topographical data.

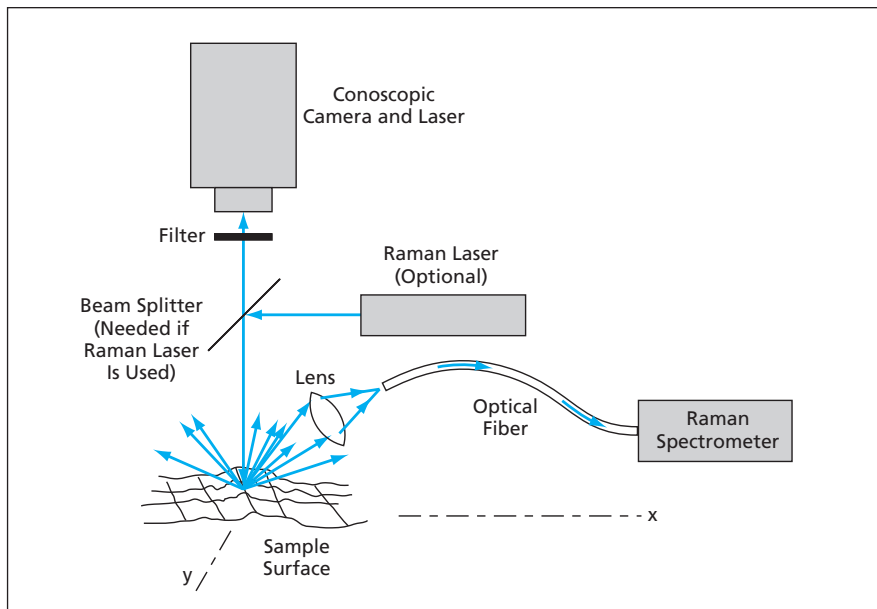
In conoscopic holography, the object and reference beams of classical holography are replaced by the ordinary and ex-

traordinary components generated by a single beam traveling through a birefringent, uniaxial crystal. In the basic conoscopic configuration, a laser light is projected onto a specimen and the resulting illuminated spot becomes a point source of diffuse light that propagates in every direction. The laser beam is raster-scanned in two dimensions ( $x$  and  $y$ ) perpendicular to the beam axis ( $z$ ), and at each  $x,y$  location, the pattern of interference between the ordinary and extraordinary rays is recorded. The recorded interferogram constitutes the conoscopic hologram. Of particular significance for the proposed instrument is that the conoscopic hologram contains information on the  $z$  coordinate (height) of the illuminated surface spot. Hence, a topographical map of the specimen is constructed point-by-point by rastering the laser beam in the  $x$  and  $y$  directions and

correlating the  $x$  and  $y$  coordinates with the  $z$  information obtained from the interferograms. Conoscopic imaging is an established method, and conoscopic laboratory instruments for surface metrology are commercially available.

In Raman spectroscopy of a surface, one measures the spectrum of laser light scattered inelastically from a laser-illuminated spot on the surface. The wavelengths of the inelastically scattered light differ from that of the incident laser beam by amounts that correspond to the energies of molecular vibrations. The resulting vibrational spectrum can be used to identify the molecules. Raman spectroscopy is a standard laboratory technique for identifying mineralogical, biological, and other specific chemical compositions.

In the design and construction of the proposed instrument, a commercially available laboratory conoscopic holographic imaging system would be integrated with a Raman spectrometer (see figure). The on-axis back-scattered laser light would be used by the imaging system to generate the conoscopic hologram of the illuminated spot. Part of the off-axis back-scattered laser light would be collected by a lens, which would couple the light into an optical fiber, which, in turn, would feed the collected light to the Raman spectrometer. The lateral ( $x,y$ ) resolution of the instrument would typically be of the order of microns, the exact value being determined primarily by the size of the laser-illuminated spot on the specimen. In one of two configurations, the Raman-excitation and conoscopic-holography beams would be generated by two different lasers and would be aligned and focused together on the same spot on the specimen. In a simpler configuration that would entail less weight, complexity,



**A Spot on a Specimen Would Be Illuminated** by a laser beam (or by two coincident laser beams) that would be raster-scanned across the surface in  $x$  and  $y$ . Laser light back-scattered from the surface would be used to map the surface height ( $z$ ) and chemical composition as functions of  $x$  and  $y$ .

size, and cost, the same laser beam would be used for both conoscopic holography and Raman spectroscopy. The two-laser configuration would be preferable in cases in which the illumination needed for Raman excitation significantly exceeds that needed for conoscopic holography and, hence, it becomes necessary to alternate between conoscopic and Raman analysis of each scan spot.

The proposed instrument would be capable of mapping topography and chemical composition at lateral scales from microns to meters, with nanometer height resolution. Thus, the instrument could provide information on composi-

tion, roughness, porosity, and fractal dimension of specimens ranging from fine dust to large rocks, without need for any preparation of the specimens. The instrument would be mechanically noninvasive in that there would be no need for mechanical contact between a solid probe and a specimen. Because the probe would be a narrow laser beam, it would be possible to profile features at the bottoms of steep, narrow holes—for instance, crevices in a rock. The proposed instrument could also be combined with other optical spectroscopic instruments.

*This work was done by Mark S. Anderson of Caltech for NASA's Jet Propulsion Lab-*

**oratory.** Further information is contained in a TSP (see page 1).

*In accordance with Public Law 96-517, the contractor has elected to retain title to this invention. Inquiries concerning rights for its commercial use should be addressed to:*

*Innovative Technology Assets Management  
JPL*

*Mail Stop 202-233  
4800 Oak Grove Drive  
Pasadena, CA 91109-8099  
(818) 354-2240*

*E-mail: iaoffice@jpl.nasa.gov  
Refer to NPO-30751, volume and number of this NASA Tech Briefs issue, and the page number.*

## Adding GaAs Monolayers to InAs Quantum-Dot Lasers on (001) InP

**Modifications enable long-wavelength lasing at higher temperatures.**

*NASA's Jet Propulsion Laboratory, Pasadena, California*

In a modification of the basic configuration of InAs quantum-dot semiconductor lasers on (001)InP substrate, a thin layer (typically 1 to 2 monolayer thick) of GaAs is incorporated into the active region. This modification enhances laser performance: In particular, whereas it has been necessary to cool the unmodified devices to temperatures of about 80 K in order to obtain lasing at long wavelengths, the modified devices can lase at wavelengths of about 1.7  $\mu\text{m}$  or more near room temperature.

InAs quantum dots self-assemble, as a consequence of the lattice mismatch, during epitaxial deposition of InAs on  $\text{In}_{0.53}\text{Ga}_{0.47}\text{As}/\text{InP}$ . In the unmodified devices, the quantum dots as thus formed are typically nonuniform in size. Strain-energy relaxation in very large quantum dots can lead to poor laser performance, especially at wavelengths near 2  $\mu\text{m}$ , for which large quantum dots are needed. In the modified devices, the thin layers of GaAs added to the active regions constitute potential-energy barriers that electrons can only penetrate by quantum tunneling and thus reduce the hot carrier effects. Also, the insertion of thin GaAs layer is shown to reduce the degree of nonuniformity of sizes of the quantum dots.

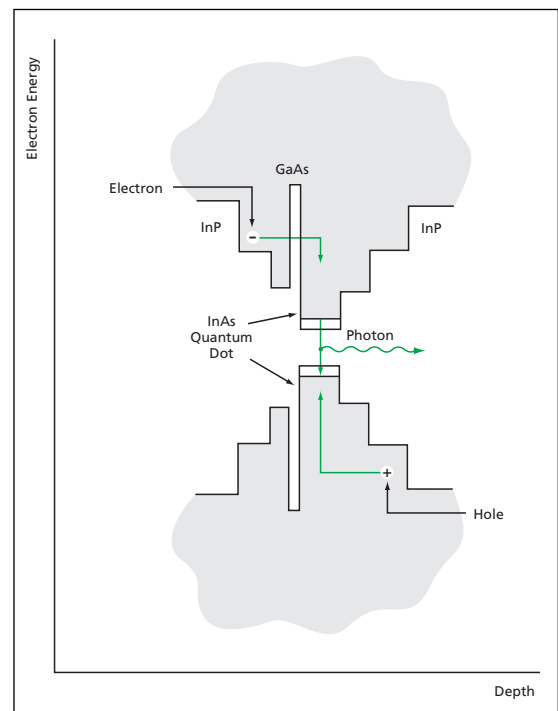
In the fabrication of a batch of modified InAs quantum-dot lasers, the thin additional layer of GaAs is deposited as an

interfacial layer in an InGaAs quantum well on (001) InP substrate. The device as described thus far is sandwiched between InGaAsP<sub>y</sub> waveguide layers, then further sandwiched between InP cladding layers, then further sandwiched between heavily Zn-doped (p-type) InGaAs contact layer.

Once a wafer comprising the layers described above has been formed, the wafer is processed into laser diodes by standard fabrication techniques. Results of preliminary tests of experimental modified quantum-dot lasers have been interpreted as signifying that these devices lase at wavelengths from 1.60 to about 1.74  $\mu\text{m}$ . The devices were found to be capable of continuous-wave operation at temperatures up to 260 K and pulse operation (duration 1 ms, repetition rate 1 kHz) at temperatures up to 280 K. It is anticipated that future such devices containing multiple stacks of quantum dots (instead of single stacks in these experimental devices) would be able to lase, at a wavelength of 2  $\mu\text{m}$ . In addition, the multiple-stack devices are ex-

pected to perform better at room temperature.

*This work was done by Yueming Qiu, Rebecca Chacon, David Uhl, and Rui Yang of Caltech for NASA's Jet Propulsion Laboratory.* Further information is contained in a TSP (see page 1).  
*NPO-40243*



**This Energy-Band Profile** of a modified  $\text{In}_x\text{Ga}_{1-x}\text{As}/\text{InP}$  quantum-dot structure shows the energy effect of the additional thin GaAs layer.

# Vibrating Optical Fibers To Make Laser Speckle Disappear

Rapid shifting of speckle makes it appear to be smoothed away.

*Goddard Space Flight Center, Greenbelt, Maryland*

In optical systems in which laser illumination is delivered via multimode optical fibers, laser speckle can be rendered incoherent by a simple but highly effective technique. The need to eliminate speckle arises because speckle can make it difficult to observe edges and other sharp features, thereby making it difficult to perform precision alignment of optical components.

The basic idea of the technique is to vibrate the optical fiber(s) to cause shifting of electromagnetic modes within the fiber(s) and consequent shifting of the speckle pattern in the light emerging from the fiber(s). If the frequency of vibration is high enough, a human eye cannot follow the shifting speckle pattern, so that instead of speckle, a human observer sees a smoothed pattern of light corresponding to a mixture of many electromagnetic modes.

If necessary, the optical fiber(s) could be vibrated manually. However,

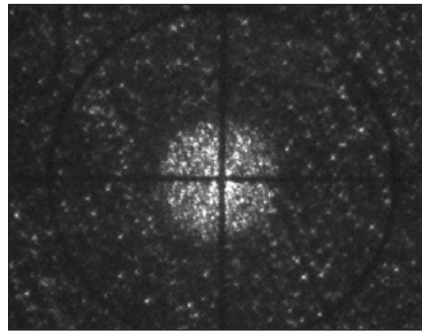


Figure 1. A **Laboratory Image** of the output of a 100-mm diameter multimode fiber is shown illuminated at 532 nm. Notice the speckle makes edges difficult to discern.

in a typical laboratory situation, it would be more practical to attach a vibrating mechanism to the fiber(s) for routine use as part of the fiber-optic illuminator. In experiments, a commercially available small, gentle, quiet, variable-speed vibratory device was used in this way, with the result that the appear-

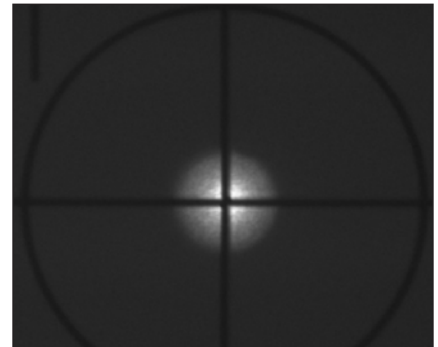


Figure 2. The **Same Image Is Improved** with the fiber being randomly vibrated. Now the edges and intensity distribution are clearly visible.

ance of speckle was eliminated, as expected. Figures 1 and 2 illustrate the difference.

*This work was done by Matthew McGill and V. Stanley Scott of **Goddard Space Flight Center**. Further information is contained in a TSP (see page 1).*

*GSC-14680-1*

# Adaptive Filtering Using Recurrent Neural Networks

Precise system models are not needed for state filtering.

Lyndon B. Johnson Space Center, Houston, Texas

A method for adaptive (or, optionally, nonadaptive) filtering has been developed for estimating the states of complex process systems (e.g., chemical plants, factories, or manufacturing processes at some level of abstraction) from time series of measurements of system inputs and outputs. The method is based partly on the fundamental principles of the Kalman filter and partly on the use of recurrent neural networks.

The standard Kalman filter involves an assumption of linearity of the mathematical model used to describe a process system. The extended Kalman filter accommodates a nonlinear process model but still requires linearization about the state

estimate. Both the standard and extended Kalman filters involve the often-unrealistic assumption that process and measurement noise are zero-mean, Gaussian, and white.

In contrast, the present method does not involve any assumptions of linearity of process models or of the nature of process noise; on the contrary, few (if any) assumptions are made about process models, noise models, or the parameters of such models. In this regard, the method can be characterized as one of nonlinear, nonparametric filtering.

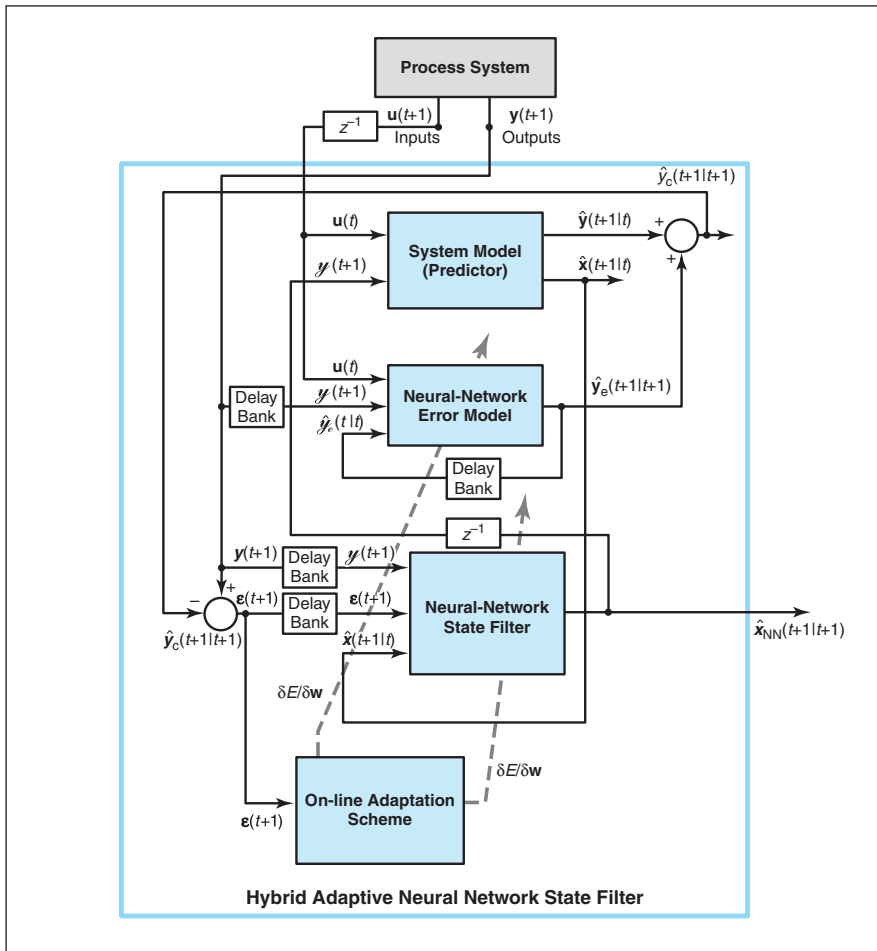
The method exploits the unique ability of neural networks to approximate nonlinear functions. In a given case, the process

model is limited mainly by limitations of the approximation ability of the neural networks chosen for that case. Moreover, despite the lack of assumptions regarding process noise, the method yields minimum-variance filters. In that they do not require statistical models of noise, the neural-network-based state filters of this method are comparable to conventional nonlinear least-squares estimators.

The figure schematically depicts an example of a process system connected to a neural-network state filter that is a hybrid of nonadaptive and adaptive parts. The nonadaptive part of the system is an available system model (predictor), which could be a conventional mathematical model or a neural network. This hybrid implementation is suitable if the inaccuracy in the system model is of a deterministic nature. The output of the system model is corrected by use of an error model implemented by a neural network. The inputs to the error model at the  $(t+1)$ st sampling time are the past inputs  $\mathbf{u}(t)$ , the past output measurements  $\mathbf{y}(t+1)$ , and the past outputs of the error model,  $\hat{\mathbf{y}}_e(t|t)$ . The output of the error model is the output correction term  $\hat{\mathbf{y}}_e(t+1|t+1)$ , and the corrected system-model output  $\hat{\mathbf{y}}_c(t+1|t+1)$  is the sum of the correction term plus the predictor output. Connection weights and biases in the error-model and state-filter neural networks are updated in response to the output residual term  $\boldsymbol{\varepsilon}(t+1) = \mathbf{y}(t+1) - \hat{\mathbf{y}}_c(t+1|t+1)$ ; the updates are generated in an on-line adaptation scheme implemented by algorithms that seek to minimize quadratic error measures by the gradient-descent method.

This work was done by Alexander G. Parlos and Sunil K. Menon of Texas A&M University and Amir F. Atiya of Caltech for Johnson Space Center. For further information, contact:

Dr. Alexander G. Parlos  
 Dept. of Nuclear Engineering  
 Texas A&M University  
 College Station, TX 77843  
 Telephone No.: (409) 845-7092  
 Fax No.: (409) 845-6443  
 Refer to MSC-22895.



A Hybrid Nonadaptive/Adaptive Neural-Network State Filter generates accurate estimates of the state of a process system, even if the system model is inaccurate.

---

## Σ Applying Standard Interfaces to a Process-Control Language

*Lyndon B. Johnson Space Center, Houston, Texas*

A method of applying open-operating-system standard interfaces to the NASA User Interface Language (UIL) has been devised. UIL is a computing language that can be used in monitoring and controlling automated processes: for example, the Timeliner computer program, written in UIL, is a general-purpose software system for monitoring and controlling sequences of automated tasks in a target system. In providing the major ele-

ments of connectivity between UIL and the target system, the present method offers advantages over the prior method. Most notably, unlike in the prior method, the software description of the target system can be made independent of the applicable compiler software and need not be linked to the applicable executable compiler image. Also unlike in the prior method, it is not necessary to recompile the source code and relink the source

code to a new executable compiler image. Abstraction of the description of the target system to a data file can be defined easily, with intuitive syntax, and knowledge of the source-code language is not needed for the definition.

*This work was done by Richard T. Berthold of Draper Laboratory for **Johnson Space Center**. For further information, contact Robert A. Brown at (617) 258-3118. MSC-22971*





National Aeronautics and  
Space Administration